View metadata, citation and similar papers at core.ac.uk

brought to you by CORE

provided by ethesis@nitr

HUMAN ADIPOSE TISSUE DERIVED ECM BASED COMPOSITES FOR TISSUE ENGINEERING APPLICATIONS

A Thesis submitted in partial fulfillment of the requirements for the degree of

Master of Technology

In

Biotechnology

By

PAMPANABOINA NARENDRA BABU
(Reg. No. 213BM2031)

Under the supervision of

Prof. Sirsendu Sekhar Ray

Department of Biotechnology & Medical Engineering

National Institute of Technology, Rourkela

Rourkela-769008, Orissa, India

June, 2015

NATIONAL INSTITUTE OF TECHNOLOGY, ROURKELA

CERTIFICATE

This is to certify that the thesis entitled "**Human Adipose Tissue Derived ECM based Composites for Tissue Engineering Applications**" by **Pampanaboina Narendra Babu** (Reg. No. **213BM2031**) submitted to the National Institute of Technology, Rourkela for the award of Master of Technology in Biotechnology during the session 2013-2015, is a record of bonafide research work carried out by him in the Department of Biotechnology and Medical Engineering under my supervision and guidance. To the best of my knowledge, the matter embodied in the thesis has not been submitted to any other University / Institute for the award of any Degree or Diploma.

Prof. Sirsendu Sekhar Ray
Assistant Professor
Department of Biotechnology & Medical Engineering
National Institute of Technology
Rourkela-769008

ACKNOWLEDGEMENTS

I would like to take the opportunity to appreciate those who played an important role in the completion of my project. With humbled feeling of gratitude, I would like to express my sincere acknowledgements to all those who directly or indirectly contributed towards completion of this endeavor. I would like to express my deep sense of gratitude and regards to my supervisor, **Dr. Sirsendu Sekhar Ray**, Department of Biotechnology and Medical Engineering for giving me an opportunity to do the project work. I acknowledge **Dr. Ajit Samal**, Super Speciality Hospital, Rourkela for gratefully providing us with human adipose tissue. I am thankful to **Prof. Indranil Banerjee**, **Prof.Thirugnanam**, **Prof. Kunal Pal**, **Prof. Devendra varma** and **Prof. Krishna Pramanik**, Department of Biotechnology and Medical Engineering, National Institute of Technology Rourkela for the valuable help and suggestions during the project work.

Further, I would like to express my thankfulness to **Mr. Joseph Christakiran M., Mr. Rik Dhar, Mr. Uvanesh kasiviswanathan** and **Ms. Priyanka Goyal**, **Ms. Alisha Prasad** for their constant support and advice in my project work. I sincerely thank all my faculty members for their blessings. Finally, I am grateful to my parents **P. Apparao** and **P. Satyavathi,** family members and friends for their endurance, love, wishes and support, which helped me in completion of my work. Above all, I thank **GOD** who showered his blessings upon us.

Pampanaboina Narendra Babu

ABSTRACT

The present study describes the preparation of extracellular matrix (ECM) based composite films, porous scaffolds, nanofibers and alginate beads for tissue engineering applications. The porous ECM-chitosan composite scaffolds were fabricated by freeze drying method for large soft tissue defects. The ECM composite injectable micro-beads were prepared by incorporating ECM within alginate by aid of centrifugal force for soft tissue engineering application. The ECM composite films were prepared by varying the ECM concentration in sodium alginate and chitosan for by solvent casting method for development of wound dressing materials. The ECM-PVA, ECM-chitosan-PVA composite electrospun fibers were fabricated using free surface electrospinning technique for use in tissue engineering applications. The interactions amongst the composites were analyzed by FTIR and XRD studies. It was noticed that the porous scaffold were bio-compatible and with increase in chitosan content the pore size decreased as observed in electron microscope. The injectable microbeads can be fabricated using a 250 μm diameter needle at 1000 rpm in bucket centrifuge, with 3 % alginate and 100 mM of calcium chloride with 0.1 % tween 80 as surfactant to reduce the coalescence of the formed beads. The films were thoroughly characterized for surface hydrophilicity, moisture retention capability, water vapor permeability, mechanical and biocompatibility. The mechanical properties suggested that the composite films had sufficient properties to be used for wound dressing applications. The ECM composite based electrospun fibers were formed at a working distance of 16cm and a working voltage of greater than or equal to 55 kV. It was noticed that with 10% PVA, and ECM concentration of 100mg/mL, with 0.02% SDS it was electrospinnable and the average fiber thickness was found to be 198±28 nm. With incorporation of chitosan, the ECM-PVA-chitosan solution was electrospinnable in 0.5M acetic acid and the average fiber thickness was found to be 356 ± 65 nm. Thus the ECM was successfully electrospun with the incorporation of chitosan and PVA to enhance the electrospinnablity of the ECM for development of ECM composite electrospun fiber for tissue engineering application.

Keywords: Human adipose tissue derived extracellular matrix, chitosan, alginate, microbeads, films, porous scaffold, free surface electrospinning, soft tissue engineering applications.

TABLE OF CONTENTS

LIST OF FIGURES

LIST OF TABLES

CHAPTER-1

INTRODUCTION

In the last decade, there has been an increase in the research on wound dressings. Wound is often described as a dynamic biosynthetic environment where a number of biological activities happen for the restoration of the loss tissues. Due to the occurrence of different biosynthetic reactions at the same time at the wound site, wound healing is often considered as a complex process. The wound healing process involves inflammation, cell proliferation and tissue remodeling[1]. The wound dressings may be broadly classified as the dry and wet wound dressings. Wet dressings have been found to be better suited for sustaining and even promoting the biosynthetic activities at the wound surface as compared to the dry dressings. [2] cell proliferation, accelerate angiogenesis, and facilitate cellular migration and epithelialization.

This helps in enhanced wound healing rate. Because of these reasons, one of the important applications of wet dressings is its use in chronic wounds. The wet wound dressings are basically polymeric architectures which have the capability to imbibe and retain [3] ECM and chitosan has received much attention as a wound dressing materials due their excellent wound healing capabilities.

Xenogenic ECM may be described as the combination of different extracellular proteins obtained from animal tissues (e.g. dermal, sub-mucosal and urinary bladder tissues of either bovine or porcine . The major components of ECM include collagen, elastin and glycosaminoglycans and supplementation of these important extracellular proteins from outside accelerate the wound healing by remodeling the tissue and acting as sacrificial template [4]**.** Additionally, ECM also contains various growth factors which enhance tissue repair by modulating the inflammatory response and promoting cell proliferation and migration [5-7].

Chitosan is a naturally occurring biodegradable polysaccharide **[8]**. N-acetyl-d-glucosamine, one of the biodegradation products of chitosan, has been found to promote fibroblast proliferation which helps in wound contraction and early stage of wound healing process. The anti-inflammatory, hemostasis and anti-bacterial property of chitosan has been found to be useful in reducing pain and preventing wound infections, thereby, indirectly helping in wound healing rate **[9]**. The properties of the chitosan wound dressings may further be improved by preparing chitosan based composite gels, films and scaffolds. The composite may be prepared using collagen **[10]**, hyaluronic acid **[11]**, silk fibroin and alginate dialdehyde **[12]**, gelatin **[13]** and heparin.

OBJECTIVES:

- To fabricate and characterize porous scaffolds for large soft tissue defects
- To fabricate and characterize injectable microbeads for soft tissue/cosmetic engineering
- To prepare and characterize composite films for wound dressing material
- To fabricate and characterize electrospun nanofibrous scaffolds

CHAPTER-2

LITERATURE REVIEW

2.1 CHITOSAN POROUS SCAFFOLDS:

The Porous chitosan scaffolds obtained from freeze drying process. The pore size will vary depends on freezing conditions[14]. The tensile strength of non porous chitosan is more than 10 times of porous chitosan, but the extensible property is twice less than porous chitosan .

Tarun garg et.al., dissolve the chitosan solution in 0.2 M glacial acetic acid and stored at room temperature for one day. Later, poured into stainless steel mould and kept in deep freezer at -70°C for 5 days. After that 5 days, mould was kept in lyophilise (Martin Christ alpha 1-2 LS plus, Germany) for 3 days.

In the lyophiliser, faced the 3 phases of preparation. First phase: freezing phase (sample was exposed up -40°C) for 10 min. Second phase: warm up vacuum pump phase (sample was exposed to -15°C) for 20 min. Third phase: drying phase (sample was exposed to 30°C) for 3 days. By following the these 3 phases, porous chitosan scaffolds can be prepared.[2]

Nitar New et.al. compared the biological and mechanical properties among the fungal chitosan scaffolds, chitosans which are obtained from shrimp and crab shells and squid bone plates. Diameter 60-90 μm observed in these scaffolds. Elongated pores observed in shrimp scaffolds but polygonal pores observed in chitosan scaffolds. Shrimp scaffolds showed that the lowest water absorption and lysozyme degradation rate whereas the fungal chitosan scaffolds showed extremely good mechanical strength, water absorption and degradation properties. The proliferation of fibroblast NIH/3T3 cells was faster with polygonal morphology on crab, squid and fungal chitosan scaffolds than shrimp chitosan. Its revealed that the fungal chitosan scaffold is the most suitable scaffold to use as a template for tissue regeneration.[3]Chitosan/gelatin prepared through formation of polyelectrolyte complex, freeze drying and post – crosslinking with glutaraldehyde. The pore diameters depends on the original water content and freezing conditions [4]. Chitosan porous scaffolds fabricated by freeze gelation method, the tensile strength and strain increased significantly in higher freezing and (1-2M) acetic acid concentration at maximum load, whereas rinse buffer with 95% ethanol concentration, tensile strength slightly increased. Crosslinking with the glutaraldehyde (GTA), enhances the tensile strength. The dose response was not observed by crosslinking with EDC and TPP [5].

Natural biodegradable polymers were processed by different techniques like novel solvent – exchange phase separation technique and thermally induced phase separation method to produce porous structures. [15].

2.2 SODIUM ALGINATE BEADS:

Alginate hydrogels extracellular matrix-like features have been key for cell delivery strategies in tissue regeneration [7]. The microbeads with simvastatin loading prepared by ionotropic gelation and cross linking technique using alginate as the hydrophilic carrier and calcium chloride as cross linking agent[16].

The blue dextran release from alginate gel beads was affected by the ratio of drying time and blue dextran/sodium alginate but not by the alginate concentration, calcium chloride concentration. The drug release was more rapid at pH 1.2 than pH 6.8.[9]

The applications of sodium alginate gel for encapsulation, immobilization of variety of cells and forms biodegradable gel when cross linked with calcium ions. Alginate as a substrate for cell proliferation until when RGD is modified. The mechanical property found high purity and high G-type alginate retained 27 % of its initial strength.[10]

The sodium alginate concentration has no effect on the release of drug like sulphamethoxazole, the release was found to be a function of calcium chloride concentration. The lower the release, the higher the concentration and smaller the water content [11].

2.3 CHITOSAN FILMS:

Chitosan films with 3 molecular weights and 4 organic acid solvents, tensile strength increased with chitosan molecular weight [12].Chitosan has a great potential for a wide range of applications due to its biodegradability, biocompatibility, antimicrobial activity, non-toxicity and versatile chemical and physical properties. Thus, chitosan based films have proven to be very effective in food preservation. The presence of amino group in C2 position of chitosan provides major functionality towards biotechnological needs, particularly, in food applications. Chitosan based polymeric materials can be formed into fibres, films, gels, sponges, beads or even nanoparticles [13].

In the chitosan films, degree of deacetylation and molecular weight affects the film properties of physicochemical. Higher the degree of deacetylation, [17]The antimicrobial and physicochemical properties of chitosan films, enhanced with essential oils (EO) , was determined invitro, showed that the antibacterial effects of the EO when incorporated in the films. The potency of antimicrobial efficacy was in order of oregano > coriander > basil > anise. With the addition of EO to chitosan films decreased tensile strength, water vapour permeability and increased in elasticity of the films.

2.4 USEFULNESS OF CURCUMIN:

Curcumin is an antibacterial pigment which is yellow in colour obtained from turmeric, rhizomes of *curcuma longa* linn (Zingiberaceae), used in medicine for the treatment of inflammatory conditions. [14]

It exhibits biological properties, anti-inflammatory, anticarcinogenic activies, hepato and nephron protective, regulates various [18].

2.5 USEFULNESS OF EXTRA CELLULAR MATRIX (ECM):

Extra cellular matrix is an acellular component present around the cells, which gives mechanical support for the cells, helps in cellular behaviours including proliferation, survival, migration and differentiation which leads to the development of cells in the tissue, possess role in signalling pathways. [11]

Four major classes of macromolecules—collagens, Glycosaminoglycans, proteoglycans, and elastin collectively comprise the ECM of mammalian cells, being both widely distributed and multifunctional throughout the body. The different types of collagen proteins available in ECM to form heterotypic fibrils to [19]. .

ECM based material scaffolds are highly compatible with tissue, possess mechanical strength which influences the cellular proliferation and cell differentiation. From the urinary bladder matrix, ECM strongly affect the smooth muscle cells phenotype, differentiation.[56] Both the tissue and scaffold possess similar compliance and should contain same mechanical property of target tissue, otherwise, it may leads to failure invivo.

CHAPTER-3

MATERIALS AND METHODS

3.1 MATERIALS:

Acetic acid was purchased from Loba Chemie Pvt. Ltd., Mumbai, India. Chitosan (Degree of deacetylation >75%), Sodium acetate trihydrate, Chloramin T trihydrate, Dulbecco's modified eagle medium (DMEM), Nutrient Broth and Fetal bovine serum (FBS) were procured from Himedia Lab. Pvt. Ltd., Mumbai, India. Citric Acid Monohydrate was purchased from SRL Ltd., Mumbai, India and 4-Dimethylaminobenzaldehyde was supplied by Merck Specialties Pvt. Ltd., Mumbai, India. Sodium Alginate was purchased from S.D.Fine – Chem. Ltd.

The Adipose derived stem cell line was procured from NCCS, Pune. All other chemicals used were of analytical grade and were obtained locally. The decllularized tissue frozen at -80^{0}C for 24hr and were lyophilized in a freeze-dryer (Operon Chemical free freeze dryer-120C).

3.2 METHODS:

3.2.1 DECELLULARIZATION OF ADIPOSE TISSUE:

The seared portions parts of the gathered adipose tissue were discard and the tissue washed in refined water for 3-4 times to evacuate the blood segments. The washed fat tisuue blended with twofold volume of refined water and homogenized in house hold blender for 5min with throb in at regular intervals. The oil removed out from the cells amid homogenization was isolated by centrifuging the suspension at 3000g for 5 min at room temperature. The upper oil layer and lower water rich layer tossed and the center layer containing fat tissue and ECM put away for further handling. The specimen after mechanical decellularization (homogenization), treated with freeze thawing method. The sample subjected to 15 cycles of stop defrosting (-20^{0}C- 37^{0}C), oil ousted after every cycles was evacuated by centrifugation at 3,000g for 5 min. After the freeze-thawing the samples were treated with anionic cleanser sodium dodecyl sulfate (SDS) to remove the oil substance furthermore help to break the plasma film and atomic layer in this way will help to content the immunogenic component DNA[20] The ECM blended in 0.5% SDS solution for 1h at room temperature. The SDS confine inside the ECM was evacuated by perpetual washing in distilled water for 24h at 4^{0}C with a water substitution in 2hr gap. The decellularized tissue was then solubilized in 0.5 M acetic acid solution under unterrupted stirring for 48 hours. The

arrangement was then sifted through muslin fabric and centrifuged again at 8000 rpm for 10 min to get absolute ECM. The ECM was then put away at 4°C for further utilize.

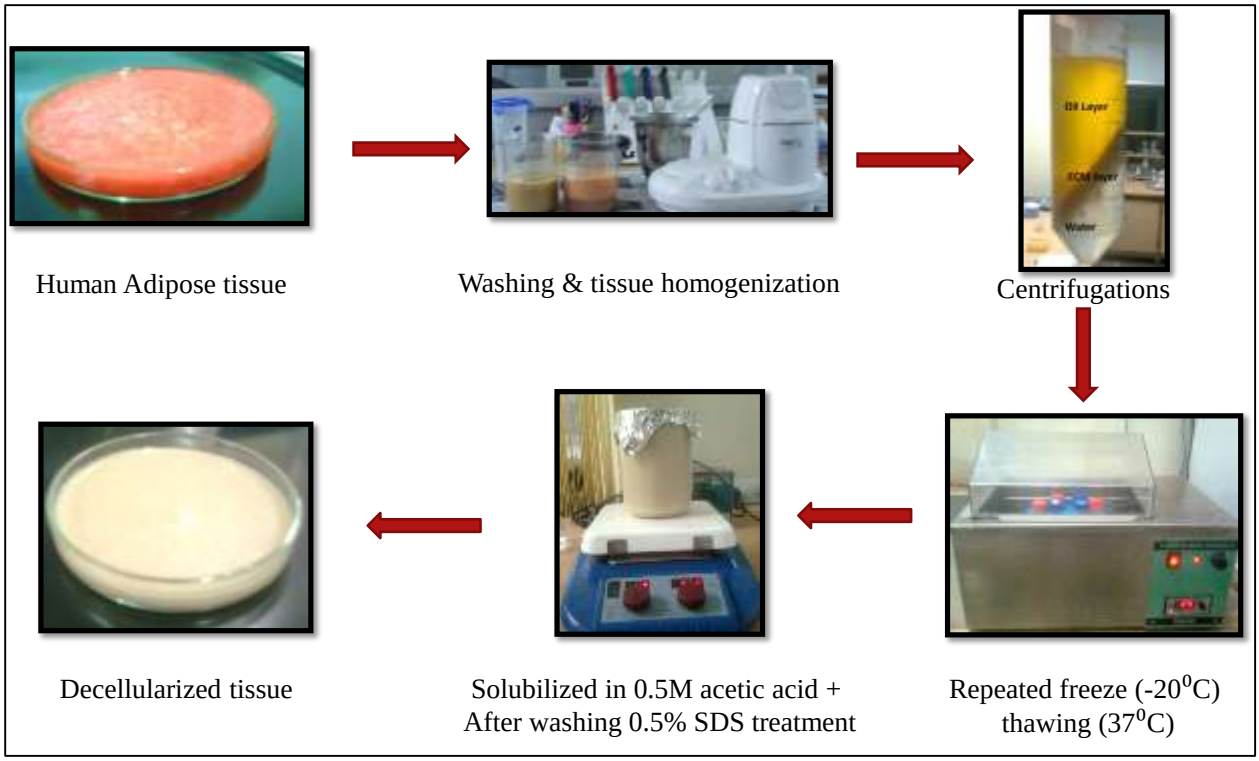

Figure – 3.1: *Decellularization of adipose tissue*

3.2.2 PREPARATION OF POLYMER-ECM COMPOSITE FILMS:

3.2.2.1 CHITOSAN-ECM COMPOSITE FILMS:

2% chitosan (Degree of deacetylation > 75%) solution was arranged in 0.5 M acetic acid solution under mixing condition. 2% alginate solution was arranged in distilled water. For which, 2gm sodium alginate powder was gradually added to distilled water under mixing condition. A Homogenous arrangement was arranged through a consistent and overnight blending. On other hand, the ECM pellet got after decellularization of omentum tissue, was lyophilized to uproot the water content from ECM pellet. From that point, lyophilized ECM was broken up in 0.5M acetic acid solution for get a definite concentration of 50 mg/ml, 100 mg/ml and 150 mg/ml. From there on, Chitosan and ECM solution (all fixations), were blended in 6:4 (w/w) proportion under blending conditions took after by degassing[21]. The chitosan-ECM composite films were prepared utilizing solvent evaporation technique as depicted by Maryam Koucha *et al.* 30g each

of prepared Chitosan-ECM arrangements were poured in the 90mm petri dish and dried for 48 hours in the vacuum oven (Q5247, Navyug, India) at 37°C. The dried composite films were extracted from petri dish utilizing 2N sodium hydroxide treatment for 30 minutes. From there on, the films were peeled out, washed 3-4 times with refined water and kept for drying at 37°C for around 24 hours.

3.2.2.2 CHITOSAN-CURCUMIN COMPOSITE FILMS:

2% chitosan (Degree of deacetylation > 75%) solution was arranged in 0.1 M acetic acid solution under stirring condition. A homogenous solution was arranged through a consistent 4 hours mixing. On the other hand, weigh the curcumin at different concentrations in 10 mg, 50 mg and 100 mg. Dissolve the curcumin in chitosan solutions by using ethanol to dissolve uniformly, with stirrer. Keep the beakers in dessicator for overnight to avoid air bubbles while pouring in petriplates. Cascade the chitosan solutions in petriplates after wiping with paraffin oil without air bubbles, such that one control, 10 mg, 50 mg, 100 mg of curcumin with films. The chitosan-curcumin composite films were concoct utilizing solvent evaporation technique as depicted by Maryam Koucha et al. 30 gm each of prepared Chitosan-curcumin solutions were poured in the 90mm petri dish and dried for 48 hours in the vacuum oven (Q5247, Navyug, India) at 37°C[22].

Figure 3.2 – *Chitosan-ECM composite film*

3.2.2.3 CHITOSAN-CURCUMIN COMPOSITE FILMS WITH GLYCEROL:

0.5% glycerol solution was prepared before adding chitosan, such that glycerol will be solubilized with chitosan more uniformly. The 2% chitosan is gradually added to distilled water under mixing condition. A homogeneous solution was prepared through a consistent and 4 hours blending. On the other hand, weigh the curcumin at different concentrations in 10 mg, 50 mg and

100 mg. Dissolve the curcumin in chitosan solutions by using ethanol to dissolve uniformly, with stirrer. The polymer solution with glycerol blended took after by degassing. 30 gm each of prepared Chitosan-curcumin solutions were poured in the 90mm petri dish and dried for 48 hours in the vacuum oven (Q5247, Navyug, India) at 37°C. The dried composite films were extracted from petri dish utilizing 2N sodium hydroxide treatment for 30 minutes. From there on, the films were peeled out, washed 3-4 times with refined water and kept for drying at 37°C for around 48 hours treatment for 30 minutes. From there on, the movies were peeled out, washed 3-4 times with refined water and kept for drying at 37°C for around 24 hours.

3.2.2.4 ALGINATE-CHITOSAN-ECM COMPOSITE FILMS:

2% chitosan solution was prepared in 0.1 M acetic acid solution under stirring condition along with 150 mg of ECM. A homogeneous solution was prepared through a consistent 4 hours blending. On the other hand, 2 % alginate solution prepared with distilled water. Keep the beakers in dessicator for overnight to avoid air bubbles while pouring in petriplates. 15 gm of alginate solution were poured in the 90 mm petri dish and leave for 12 hours in vacuum oven (Q5247, Navyug, India) at 37°C. After 12 hours, 15 gm of chitosan solution with ECM poured over the layer of alginate film in petri dish and dried for 48 hours in vacuum oven, such that the crosslinking impact will be more. Along with these films, the control films of each 30 gm also prepared of alginate, chitosan, and alginate chitosan composite films[23].

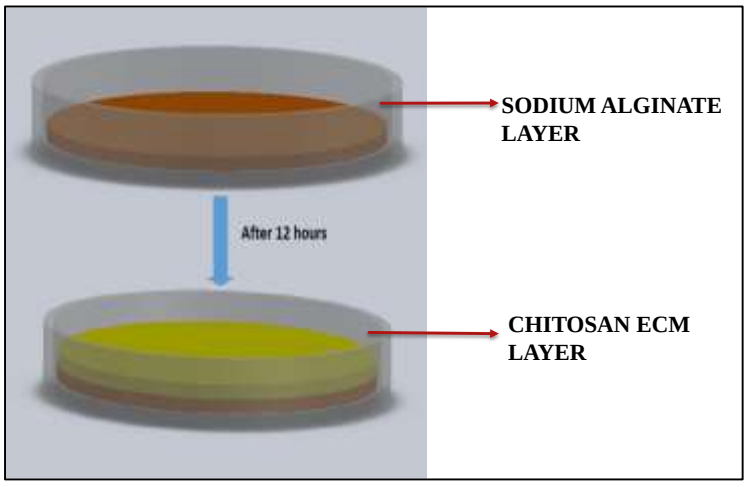

Figure 3.3 – *Layer by layer approach to fabricate polyelectrolyte ECM composite films*

3.2.3 PREPARATION OF ALGINATE-ECM COMPOSITE MICROBEADS:

2 % alginate solution was prepared with 1 mg/ml of ECM in distilled water under stirring condition. For formation of specific size of beads, prepared 100 mM of calcium chloride solution was added with 0.1% of tween 80 to reduce the random size of beads. The beads were performed by falcon tubes centrifugation through bucket centrifuge with needle and syringe. The setup was arranged by inserting syringe in falcon tube in such a way that there should be a gap between needle and calcium chloride solution. Centrifugation was carried out in 1000 rpm to execute best beads without any tailor cones[24].

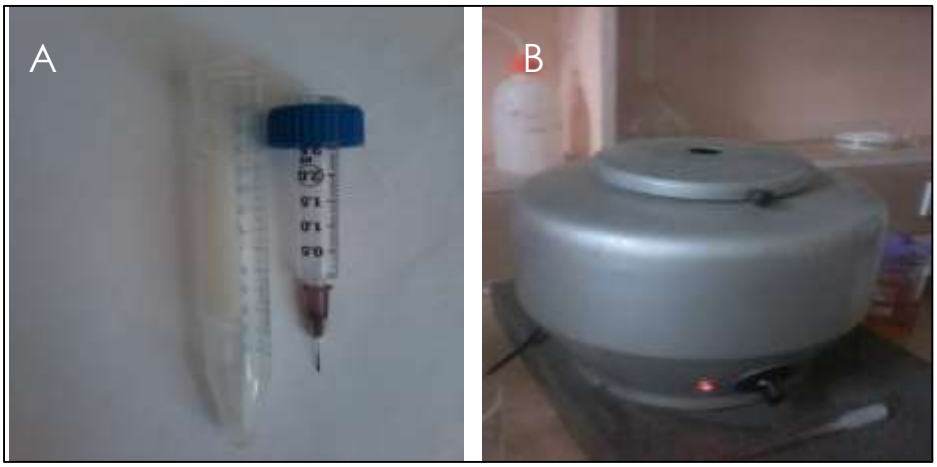

Figure 3.4 - *A) Falcon tube with needle B) Bucket Centrifuge*

3.2.4 PREPARATION OF CHITOSAN-ECM POROUS SCAFFOLD:

ECM was blended with distilled water, 0.1 % chitosan is gradually added. On the other hand, the other ECM with 1% chitosan is prepared. The prepared solution fabricated into 3 dimensional scaffolds with a certain mould with freeze drying method.

Figure 3.5 – *Freeze dried porous scaffold with mould*

3.2.5 PREPARATION OF ELECTROSPUN ECM COMPOSITES:

2 % chitosan solution was prepared in 0.5 M acetic acid solution. On the other hand, 100 mg/ml of ECM solution was prepared in distilled water with 10 % polyvinyl acrylamide. Both the solutions were mixed in ratio of 30:70 with ECM PVA solution and chitosan respectively. Electrospinning was carried out in Roller Electrode Electrospinning or free surface electrospinning[25].

3.2.6 CHARACTERIZATION OF ECM COMPOSITES:

3.2.6.1 MECHANICAL TESTING OF FILMS:

The mechanical properties of the Chitosan ECM films, chitosan curcumin films and alginate chitosan ECM composite films were analyzed using stress relaxation and creep recovery studies. The tests were conducted using a static mechanical tester (TA-HD plus Texture Analyzer, Stable Micro Systems, UK). The films were cut into rectangular pieces of size 5 mm x 60 mm. The films were held using tensile grip attachment such that the length between the probes was 50 mm (effective length). For the stress relaxation study, the films were stretched by 1 mm after a trigger force of 5 g. The relaxation study was conducted for a period of 60 s. The creep study was conducted by applying a force of 50 g during the creep phase and subsequently applying a force of 5 g during the recovery phase. The mechanical testing was done using the two models as discussed in the Figure 3.6, with the various parameters discussed in the results and discussions section.

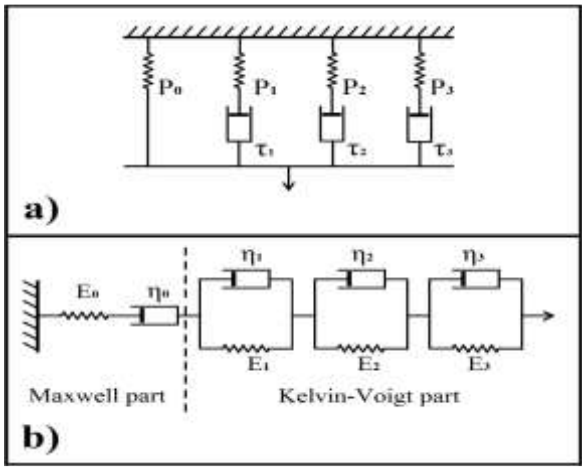

Figure 3.6 - *Mechanical testing models -a) Weichert Model, b) Burger's model*

3.2.6.2 X-RAY DIFFRACTION:

The prepared composites were analyzed using X-ray diffractometer (PW3040, XRD-PANalytical, Philips, Holland). Cu – Kα radiation (0.154 nm) was performed. The instrument was operated at 30 kV and 20 mA. Scanning of the films was done at 5° - 50° 2θ at a rate of 2° 2θ /min, porous scaffolds was done at 5° - 40° at a rate of 5° 2θ /min, and the beads was done at 5° - 45° at a rate pf 5° 2θ /min. The analysis was performed at the room-temperature.

The crystallinity index (Cr_I) of the films was calculated from the diffractograms using following equation:

$$Cr_I = \frac{(I_{21} - I_{16})}{I_{21}}$$

where, I_{21} is the intensity of peak at 21° 2θ; and I_{16} is the intensity of the amorphous valley peak at 16° 2θ.

3.2.6.3 FOURIER TRANSFORM INFRARED SPECTROSCOPY:

The prepared composites were analyzed using FTIR spectroscope to understand the interaction The spectroscope was operated in the ATR mode (Alpha-E, Bruker, Germany). Scanning was done in the wavenumber range of 4000 cm^{-1} to 500 cm^{-1}.

3.2.6.4 SURFACE HYDROPHILILICITY:

The surface hydrophilicity of the chitosan ECM films was measured using the sessile drop method. Drop of water was placed on the rectangular pieces of the composites and the contact angles were obtained using drop shape analyzer (DSA 25 Kruss Germany).

3.2.6.5 MOISTURE ABSORPTION TEST:

For the moisture absorption tests, the films were cut into pieces of 1 cm x 1 cm and subsequently dried in a vacuum drying oven for 24h. The films were weighed and then transferred to a desiccator, maintained at 84% humidity using saturated solution of potassium chloride, for 12h. The final weight of the films was noted. The percentage of moisture absorbed was calculated using equation:

$$\%M = \frac{W_f - W_i}{W} \times 100$$

where, %M= Percentage of moisture absorbed, W_i= Initial weight of the films; and W_f = Final weight of the films after incubating in the desiccator.

3.2.6.6 WATER VAPOR TRANSMISSION TEST:

Water vapor transmission of the films was evaluated as per the ASTME 96 standard. In brief, the chitosan ECM composite films and chitosan alginate ECM films were kept completely adhered on the top of the cylindrical glass tubes (volume = 71.42 cm^3) using a Teflon tape (P.T.F.E. Thread Seal Tape). The arrangement of the complete setup has been illustrated in Fig. S1. Each tube was initially filled with preweighed (30 ml) PBS. The initial weight and height of the water (from base) was recorded and then the tubes were kept at 37 °C. The readings were taken at regular intervals of 2 days for two weeks. The transmission of water vapor through the films was calculated using following equation:

$$WVTR = \frac{B_2 - B_1}{t} \times A$$

where, WVTR=Water vapor transmission rate (g/day-m^2); B_2= Final weight of the set-up; B_1= Initial weight of the set-up; t= Time (days); and A= Effective area of evaporation.

3.2.6.7 CURCUMIN RELEASE KINETICS:

The polymer – curcumin composite films were analyzed for the drug release kinetics. The films were placed in a PBS solution and covered with dialysis membrane. The constant volume of PBS was taken at regular intervals of time of 15 min, 30 min, 45 min, 1 hr, 2 hr, 3 hr, 4 hr, 5 hr, 6 hr, 8 hr, 12 hr, 24 hr, 48 hr, 72 hr, 96 hr, 120 hr, and 144 hr. While taking the readings each time, the volume was maintained constant by replacing it with fresh PBS such that to add cumulatively from time to time. The absorbance of all the samples was taken at 430 nm [150].

3.2.6.8 CONFOCAL MICROSCOPY:

The presence of ECM in the micro-bead composites were found using the dye ANS (8-Annilino-napthalene sulfate), which detects the surface hydrophobicity of the proteins. Using Leica TCS

SP8 confocal microscope, the ANS dye was incubated with beads and with an excitation of 390nm the presence of protein was detected.

3.2.6.9 SCANNING ELECTRON MICROSCOPY OF POROUS SCAFFOLD:

Scanning Electron Microscopy (SEM) was performed utilizing a JEOL-JSM 6480 LV to discern the morphology of chitosan ECM porous composite scaffolds, alginate beads, electrospinned fibers at both cross-segment and longitude-area. Platinum covering was done preceding imaging.

3.2.6.10 HEMOCOMPATIBILITY TEST:

For hemocompatability studies of chitosan curcumin composite films, the fresh goat blood was taken and diluted in 1:1 ratio with 0.9 % normal saline and 0.5 ml of dilute blood. The dried films cut in size ($1*1cm^2$) placed in saline for 1 hr. After taking of diluted blood with saline and blood in 5:4 ratio respectively, for making of positive control, add 0.5 ml of blood and make upto 10 ml of saline. For negative control, add 0.5 ml of 0.01N HCL and make upto 10 ml with saline. The percentage of hemolysis can be calculated by using the formula.

$$\mathbf{Z\ \% = ((D_t - D_{nc})/\ (D_{pc} - D_{nc}))*100}$$

Where, D_t = test OD, D_{nc} = OD of negative control, D_{pc}= OD of positive control. If the percentage is more than 5, it is haemolytic. If 2 to 5 it is slightly haemolytic and if it is found between 0 to 2 non-hemolytic in nature.

3.2.6.11 *IN-VITRO* CYTOTOXICITY TESTS:

The ability of the chitosan ECM composite films, chitosan curcumin films, Alginate chitosan ECM composite films, porous scaffolds and sodium alginate beads to support the proliferation of the human subcutaneous adipose tissue derived stem cells (ADSCs) was evaluated *in vitro*. The ADSCs were procured from Himedia Pvt. Ltd. Mumbai, India after Institute ethical clearance. The cells were maintained in Dulbecco's Modified Eagle Medium (DMEM) with 10% Fetal Bovine Serum (FBS) at 37 °C (5% CO_2 and 95% humidity)[26]. The media was replaced every 72h.When the cells reached 80% confluency, they were harvested with 0.05% trypsin/EDTA

solution. Subsequently, the cells were seeded at a cell concentration of (1×10^4) cells/ml onto 24 well plates. After 24h of incubation, the status of cell adherence were evaluated and ethanol sterilized film samples (1cm x 1cm) were added into the wells. The metabolic activity of cells was monitored using MTT assay after 48h of incubation .The assays were done in quadruplet for each sample.

3.3 STATISTICAL ANALYSIS:

The statistical analysis of the experimental data was carried out by unpaired t-test and one – way ANOVA using IBM SPSS Statistics 20.0. The p values of ≤ 0.05 were considered to be statistically significant.

CHAPTER-4

RESULTS AND DISCUSSION

4.1 PREPARATION AND CHARACTERIZATION OF COMPOSITE FILMS:

4.1.1 CHARACTERIZATION ECM-CHITOSAN FILMS:

The ECM was incorporated within the chitosan films so as to accelerate the wound healing process. It was expected that the presence of collagen, elastin and glycosaminoglycans might enhance the rate of wound healing. Also, it was expected that the ECM derived from the omentum might be a rich source of growth factors due to the high vascularization of the omentum tissue. Apart from the above, during the extraction of the ECM, it was observed that a very good proportion of ECM was extracted using a relatively simple process of combination of mechanical thermal and chemical methods. The prepared films were light brown in color. This was mainly due to the color of the chitosan. The films were translucent in nature. The total collagen content of the digests was determined using the relationship that hydroxyproline forms 14.3% of total collagen. The extracted collagen contents of the omentum derived ECM was determined to be 0.78 ± 0.07 mg of collagen per mg of initial dry weight.

4.1.1.1 MECHANICAL ANALYSIS OF ECM-CHITOSAN COMPOSITE FILMS:

The mechanical properties of the films were analyzed by conducting stress relaxation and creep-recovery studies. During the loading phase of the stress relaxation study (as seen in Figure 4.1), the force was monotonously increased till the end of the loading phase. Thereafter, there was a decrease in the force to a residual value due to the molecular rearrangement of the polymeric chains in the films. The maximum force at the end of the loading phase is regarded as F_0, which provides the information about the firmness of the films. It was observed that the incorporation of ECM resulted in the decrease in the firmness of the films. Amongst the ECM containing films, there was an initial decrease in the firmness of the films when the ECM content was increased from CE50 to CE100. Thereafter, a further increase in the ECM content resulted in the increase in the firmness of the films. D_{300} was calculated to have an understanding on the ductility of the films. D_{300} is defined as the distance moved by the probe to attain a 300 g force. From the results (Table 4.1), it was seen that the ductility of CE100 was highest.

Table 4.1 - *Mechanical properties of the films based on stress relaxation studies*

Sample	Un-normalized curve			Normalized Curve			
	F_0	F_r	%relaxation	D_{300}	K_1	K_2	R^2
CC	676.2	302.0	55.3	0.31	0.01	-0.038	0.998
CE50	530.6	301.0	43.2	0.27	0.01	-0.057	0.996
CE100	373.4	255.3	31.6	0.40	0.01	-0.061	0.996

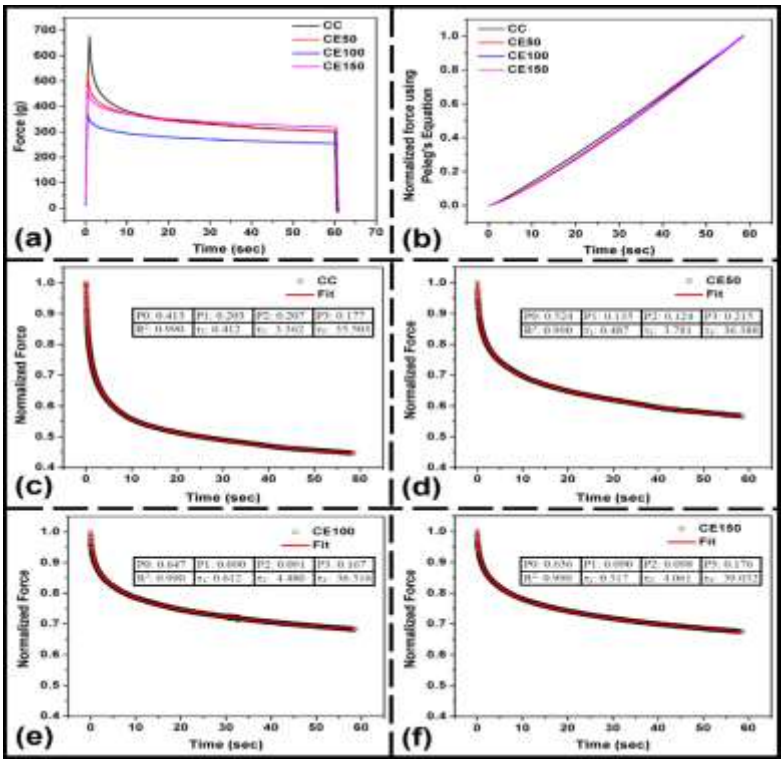

Figure 4.1 - *(a) Stress relaxation profiles; (b) Stress relaxation curves after fitting to the modified Peleg's equation; (c-f) Weichert model fitting curves to the stress relaxation profiles.*

For a composite film to be used as a wound dressing material, the ductility of the material is an important criterion. Hence, it is expected that CE100 might be a comparatively efficient film for wound dressing. The trend of the residual force (F_r) of the films was same as that of the maximum force during the loading phase. The residual force is an indicator of the energy stored in the films after the relaxation process. From the maximum loading force and the residual force, percent relaxation (%SR) was calculated. It was observed that the %SR was highest in the

control. Amongst the ECM containing films, the %SR was highest in CE50. The %SR of CE100 and CE150 was nearly equal. Higher stress relaxation values of control and CE50 suggested that these films were having higher viscoelastic fluid nature. In other words, the viscoelastic solid component was predominant in CE100 and CE150.

The viscoelastic property of the films was predicted using modified Peleg's equation [26]. The constants K_1 and K_2 are the indicators of initial rate of relaxation and the extent of relaxation, respectively. The K_1 values of all the films were similar. This suggested that the initial rate of relaxation was nearly equal in all the films. The K_2 values were found to be lower in the films with higher proportion of ECM. This observation is in accordance to the %SR values obtained from the stress relaxation profile. The Peleg's equation is given as follows:

$$P_{(t)} = P_{(0)} + P_{(1)}.e^{\left(\frac{-t}{\tau_1}\right)} + P_{(2)}.e^{\left(\frac{-t}{\tau_2}\right)} + P_{(3)}.e^{\left(\frac{-t}{\tau_3}\right)}$$

Unfortunately, the Peleg's model also failed to explain the viscoelastic properties of the films in-depth. Hence Weichert mechanical model (Figure 4.2) for viscoelasticity was used for predicting the viscoelastic behavior of the films. The Weichert model is the most commonly used model for understanding the viscoelastic property of soft materials. The experimental data were fitted to the Weichert model by non-linear least square sum of difference method. The correlation coefficient between the experimental data and the fitted data was >0.98. This suggested a close match between the experimental and the fitted data. P0 provides information about the modulus of elasticity of the Hookean spring in the Weichert model. This factor provides information about the inherent elasticity of the viscoelastic materials. It was found that there was an increase in the P0 values when the ECM content was increased from control to CE100. Thereafter, there was a slight reduction in the P0 value in CE150. These results are in accordance with the %SR values where it was observed that the %SR was lowest in CE100, which indicates that the elastic component of CE100 was higher. The P1 value indicates the initial elastic value during the relaxation process. A decrease in the P1 values was observed with the increase in the ECM content. The P1 values of CE100 and CE150 was equal. τ_1 value was increased with the increase in the ECM content till CE100. Subsequently, a further increase in the ECM content in CE150 resulted in the decrease in the τ_1 value. τ_1 value is a marker of the initial relaxation time during

the relaxation process. This suggested that the relaxation process in CE100 was slowest and may be accounted to the interaction of the proteins molecules present in the ECM with the chitosan molecules. The τ_2 values also followed the same trend as that of τ_1. τ_3 showed an increase in the relaxation time with the increase in the ECM content. τ_2 is an indicator of the intermediate relaxation process, whereas, τ_3 is a marker of the relaxation process happening at longer period of time after the load has been applied. The occurrence of the intermediate (τ_2) and the delayed (τ_3) relaxation time have been reported to be associated with the breakage of the polymer-polymer interactions in the films. The analysis of τ_2 and τ_3 suggested that the breakage of the polymer-polymer interactions was much lower in CE100. Hence, it is expected that CE100 might maintain its integrity in case of sudden accidental stress being applied.

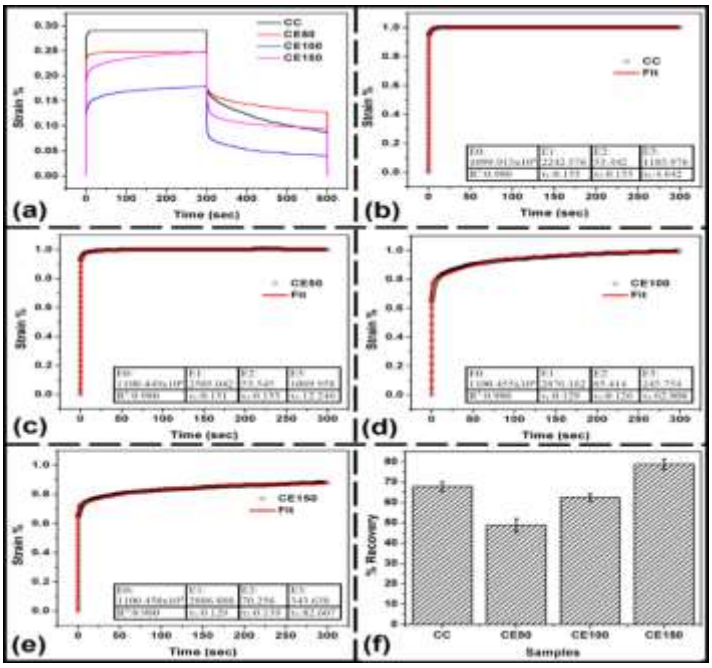

Figure 4.2 - *(a) Creep recovery profiles of the films; (b-e) Burger's model fitting curves to the creep data and (f) % recovery of the films.*

The creep study (Figure 4.2) is associated with the application of a constant load for a particular period of time. The cumulative strain developed during this period is recorded. This gives information about the ability of the films to undergo molecular rearrangement when a constant force is applied. The analysis of the creep data was done by fitting the experimental data to the eight-element Burger's model.

Table 4.2 - *Mechanical properties of the films based on creep studies*

Sample	η_0	η_1	η_2	η_3
CC	3.12E+09	343.2282	8.176258	5505.177
CE50	3.11E+09	329.2308	7.114436	13102.45
CE100	3.11E+09	371.0418	8.262875	15435.28
CE150	3.11E+09	373.3812	9.775125	28386.88

In many cases, it has been seen that either four-element or six-element Burger's model is sufficient to model the creep properties of the soft materials. But in this case, an eight element Burger's model was needed to efficiently model the creep data. The instantaneous elasticity (E0) was found to be higher in ECM containing films. This indicated that the addition of ECM to the chitosan matrix helps improving the instantaneous elastic component of the chitosan films. The initial elastic (E1) and the intermediate elastic (E2) components, during the loading phase, also showed a similar trend, i.e., an increase in the elastic component with the increase in the ECM. On the contrary, the delayed elastic component (E3) showed a reverse trend. The initial and the intermediate relaxation time of the control film were higher than the ECM containing films. Amongst the ECM containing films, both the initial and the intermediate relaxation times initially decreased with the initial increase in the ECM content in CE100. A further increase in the ECM content increased the relaxation time. The delayed relaxation time was found to be higher in the films with higher ECM content. An increase in the delayed relaxation time with the ECM content suggested that the incorporation of ECM in the chitosan matrix retarded the breakage of the polymer-polymer interactions. The percentage recovery of the ECM containing films was found to be higher in the films containing higher amount of ECM. This indicated that an increase in the ECM content might result in the increase in the viscoelastic fluid component. To have an insight on the viscous components of the dashpots of the Burger's element was calculated. It was found that the instantaneous viscosity of the films were much higher. Except the instantaneous viscosity, the viscosity of the other dashpots (associated with the Kelvin-Voigt parts) showed an increase in the viscosity with the increase in the ECM content.

The %SR studies indicated that when an instantaneous stress is applied to CE100, the chances of breakdown of the polymer-polymer interactions are lower. On the contrary, the creep study suggested that when a constant load is applied on the films the chances of breakdown of the polymer-polymer interactions is lower in the films with higher ECM content. From the above, it can be concluded that CE100 might have sufficient properties to be used as wound dressing materials.

4.1.1.2 XRD AND FTIR ANALYSIS OF THE ECM-CHITOSAN FILMS:

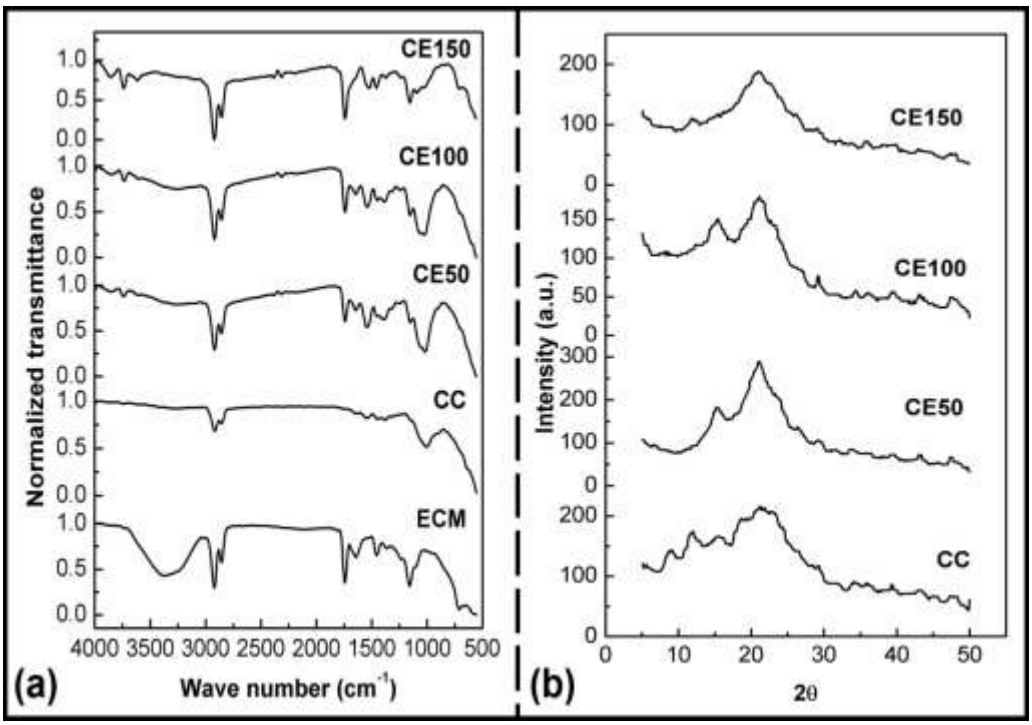

Figure 4.3 – *XRD and FTIR Spectrographs of ECM-Chitosan films*

The X- ray diffractograms of chitosan and the films have been shown in Figure 4.3. X'Pert High score (Version 1.0b, Philips analytical B.V) was used to analyze the diffractograms of the films. Chitosan has been reported to have diffraction peaks at ~10° and ~20° 2θ [27]. Collagen, a major constituent of ECM, shows a broad diffraction pattern at 10° 2θ along with a characteristic peak at 23° 2θ [28]. The typical peaks (12° 2θ and 21° 2θ) of chitosan were noticed in the composite films. A decrease in the intensity of the peak at 12° 2θ with the corresponding appearance of a new peak at 15° 2θ was observed in the chitosan films. An increase in the crystallinity index (Table 4.3) was observed in CE50, which gradually decreased with the increase in the ECM in

the films (CE100 and CE150) as compared to the chitosan film (CC).Crystallinity of biopolymers plays important role in modulating their mechanical and biological properties. In general, with increase in crystallinity, tensile strength and stiffness increases and creep decreases. But increase in crystallinity also imparts anisotropy to a composite structure. Increase in crystallinity is also been associated with lower inflammatory response and higher cell adhesion.

Table 4.3: *Crystallinity index of the films*

Samples	**Crystallinity index**
CC	0.28
CE50	0.43
CE100	0.36
CE150	0.35

The FTIR analysis was done to have an understanding about the chemical interactions amongst the components of the chitosan-ECM composite films. The major absorption peaks associated with the chitosan include 3428 cm^{-1} (N-H and O-H stretching), 2949 cm^{-1}(CH_3 symmetric stretching), 1663 cm^{-1} (C=O stretching vibrations), 1439 cm^{-1} (C–N stretching vibration), 1365 cm^{-1} (CH_3 bending vibration), 1134 cm^{-1} (C–O–C bending vibration), and 1084 cm^{-1} (C–OH stretching vibration) [41]. As discussed above, ECM is mainly a mixture of various proteins. Hence, the FTIR spectra of ECM was expected to have amide I (1622 cm^{-1}, 1630 cm^{-1}, 1638 cm^{-1}, and 1644 cm^{-1}), amide II (1552 cm^{-1}, 1560 cm^{-1}, and 1579 cm^{-1}) and amide III (1259 cm^{-1}) bands. These absorption peaks were also observed in the prepared films. Absense of any new charactereistic peaks suggested that there was no new bond formation and hence the interaction amongst the ECM and chitosan.

4.1.1.3 SURFACE HYDROPHILLICITY:

Contact angle measurement data (Fig. 4a) indicate that there is statistically significant increase in hydrophilicity of the ECM containing films compared to chitosan only film. Furthermore, CE50,

CE100 and CE150 have statistically significant difference in the contact angles signifies with increase in the concentration of ECM in chitosan film, the hydrophilicity keeps increasing.

4.1.1.4 MOISTURE ABSORPTION:

In concordance with the increasing hydrophilicity of composite films, the moisture absorption capacity of the films (Fig. 4b) was lower in the films which contained lower proportions of ECM. The differences in the absorbed moisture amongst the films were statistically significant. The components (e.g. collagen, elastin and glycosaminoglycans) of ECM are proven hydrophilic molecules. Hence, incorporation of ECM into the films resulted in the increase in the hydrophilicity of the films, which in turn, resulted in the absorption of higher amount of moisture.

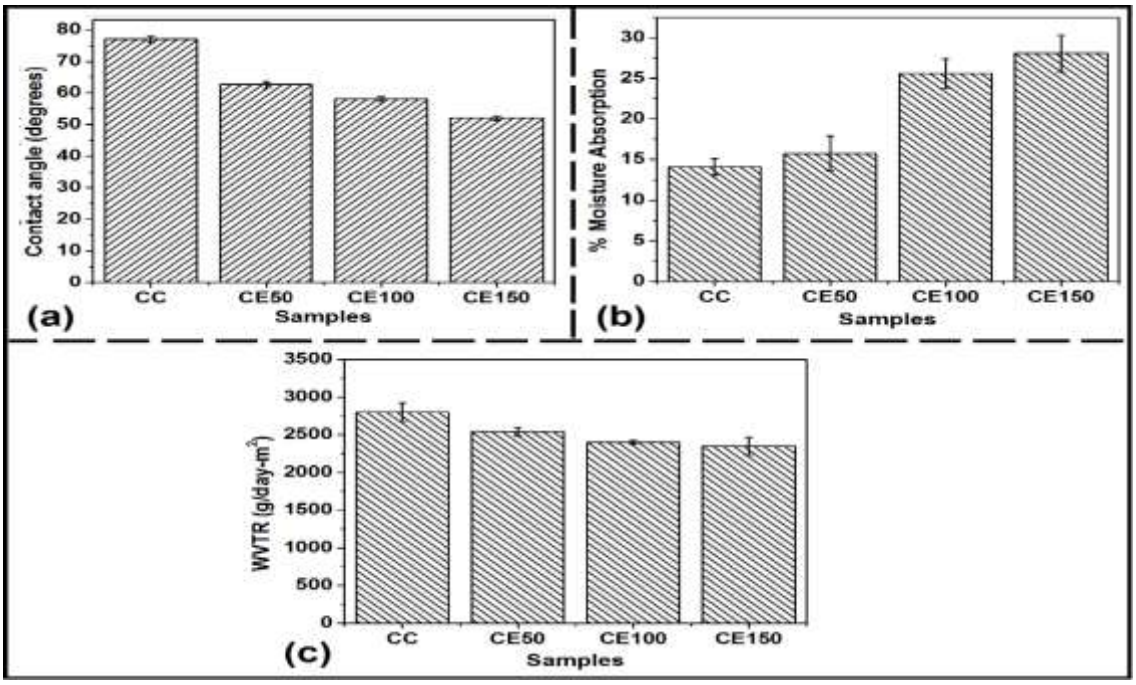

Figure 4.4 – *a) Surface hydrophobicity, b) Moisture adsorption and c) water vapor transmission*

4.1.1.5 WATER VAPOR TRANSMISSION TEST:

Water vapor transmission rate (WVTR) is regarded as the transmission of the water vapor per unit time through a unit area of the materials under test. The water vapor transmission rate (Fig. 4c) was determined. The differences observed amongst the different groups were statistically significant. An increase in the ECM concentration resulted in the decrease in the WVTR. This can be explained by the increase in the hydrophilicity of the films when ECM was incorporated,

which resulted in the increase in the binding of the water molecules. This, in turn, resulted in the decrease in the permeability of the water vapor from the films.

An ideal wound dressing should control the water loss at an optimal rate and keep the wound moist. The recommended rate of water loss in the form of vapor is 2000–2500 g/day-m^2 [29]. This rate of evaporation is expected to keep the wound moist without getting dehydrated. The WVTR though the composite films falls within the recommended range indicating its suitability as better wound dressing material.

4.1.1.6 *IN VITRO* CYTOTOXICITY TEST:

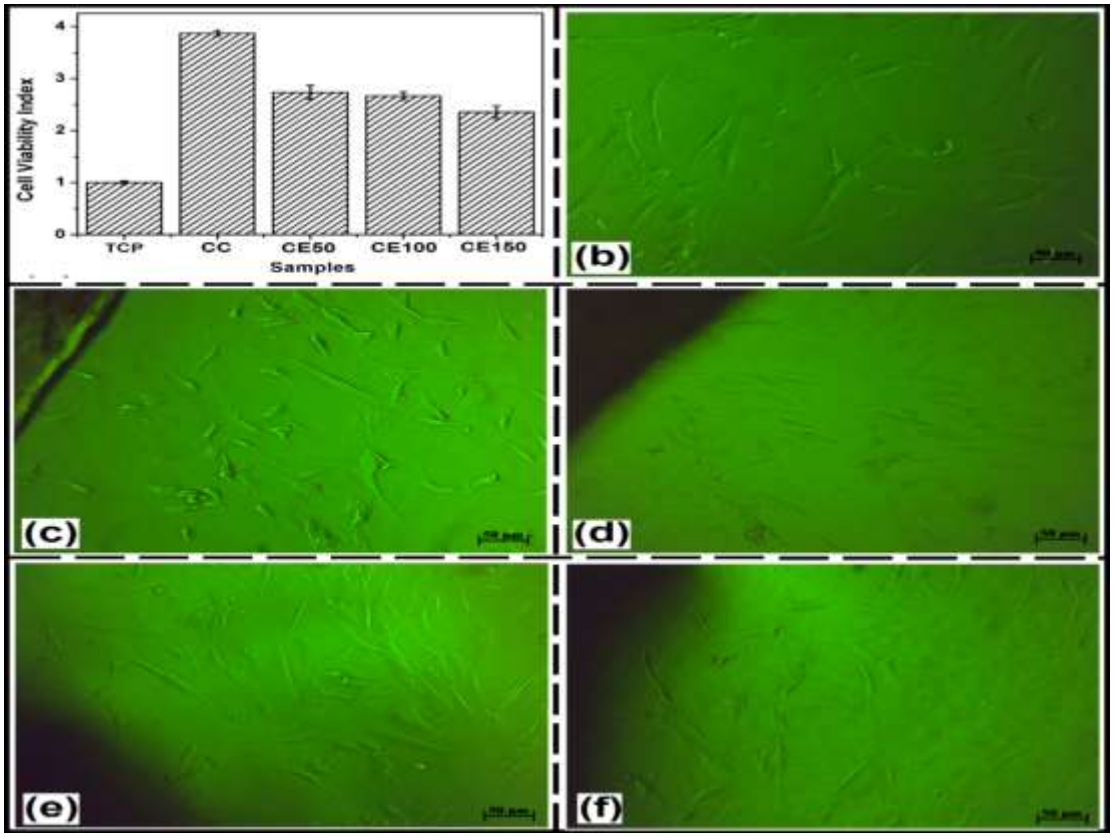

Figure 4.5 – *In vitro cytotoxcity test using MTT for chitosan-ECM films*

The *in vitro* cytocompatibility of the films was analyzed using the MTT assay (Figure 4.5). All the films were found to be cytocompatible. The chitosan film and the chitosan-ECM composite films showed statistically significant increase in cellular proliferation when compared to the cells grown on tissue culture plate (control). The chitosan film (CC) showed better cellular

proliferation as compared to the composite films. However, increasing the concentration of ECM in the composites, revealed no statistically significant increase in the cellular proliferation. The micrographs of the adipose derived stem cells indicate that the spreadability of individual cells in presence of composite films was higher than the chitosan film. The presence of protein 4.1 superfamily in extracellular matrix is known to increase the spreadability of the cells through integrin family receptor binding and β-integrin mediated cell spreading [30]. The results indicated that the developed composite films were well suited for wound healing applications.

4.1.2 CHARACTERIZATION CHITOSAN-CURCUMIN AND CHITOSAN-CURCUMIN-GLYCEROL FILMS:

4.1.2.1 MECHANICAL ANALYSIS OF THE FILMS:

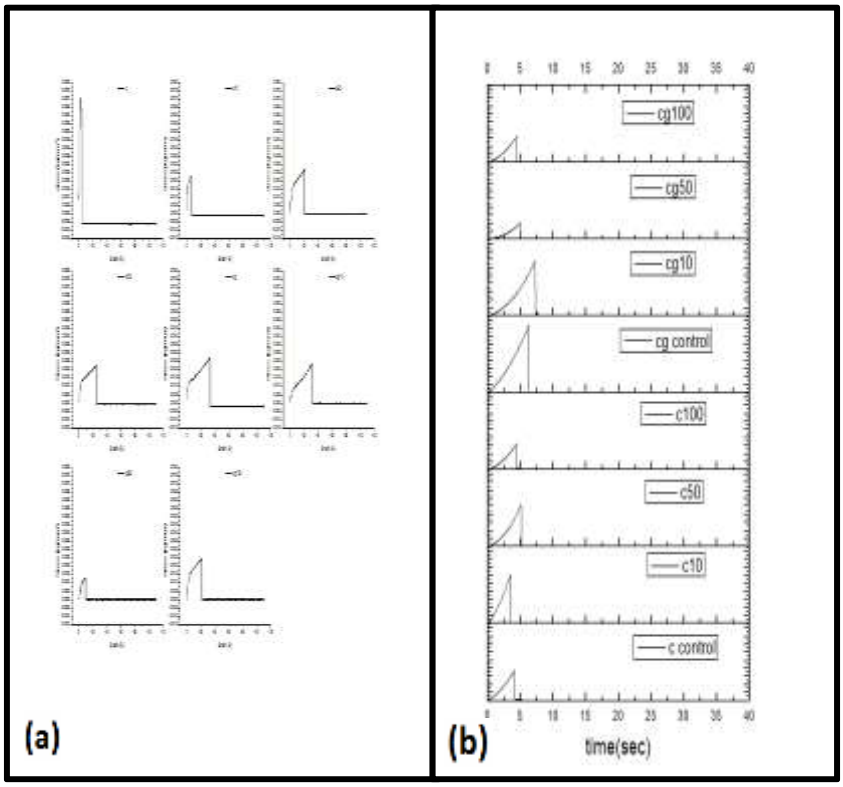

Figure 4.6 – *Mechanical analysis of curcumin-chitosan and curcumin-chitosan-glycerol films*

Table 4.4 – *Toughness and Ultimate bursting strength of composite films*

Sample	Area under curve	Ultimate bursting strength	Time at bursting (sec)
C control	6023.55	3689.27	4.11
C10	6064.220	6064.220	3.5
C50	9534.27	5199.192	5.165
C100	5057.223	3213.302	4.43
CG	21773.69	8332.082	6.325
CG10	17351.233	6831.453	7.3
CG50	3296.021	2016.275	5
CG100	4977.348	3227.766	4.43

The area under the curve from figure 4.6a, signifies the toughness of the films. The toughness of the films increases with increase in curcumin in the composites. The ultimate bursting strength decreased with increasing concentration of curcumin, suggesting curcumin had a role to play in the mechanical stability of the films.

4.1.2.2 XRD AND FTIR ANALYSIS:

Chitosan has been reported to have diffraction peaks at ~10° and ~20° 2θ and all the composites had the characteristic peaks of chitosan in the diffractogram. With increase in concentration of the curcumin concentration the amorphous nature of the chitosn increased which is evident with the decrease in crystallinity. The FTIR analysis was done to have an understanding about the chemical interactions amongst the components of the chitosan-curcumin composite films. The major absorption peaks associated with the chitosan include 3428 cm^{-1} (N-H and O-H stretching), 2949 cm^{-1}(CH_3 symmetric stretching), 1663 cm^{-1} (C=O stretching vibrations), 1439

cm^{-1} (C–N stretching vibration), 1365 cm^{-1} (CH_3 bending vibration), 1134 cm^{-1} (C–O–C bending vibration), and 1084 cm^{-1} (C–OH stretching vibration). Peak shifts were noticed around 1439 cm^{-1} (C–N stretching vibration), 1365 cm^{-1} (CH_3 bending vibration), 1134 cm^{-1} (C–O–C bending vibration), and 1084 cm^{-1} (C–OH stretching vibration) suggesting possible interaction of curcumin with the chitosan functional groups

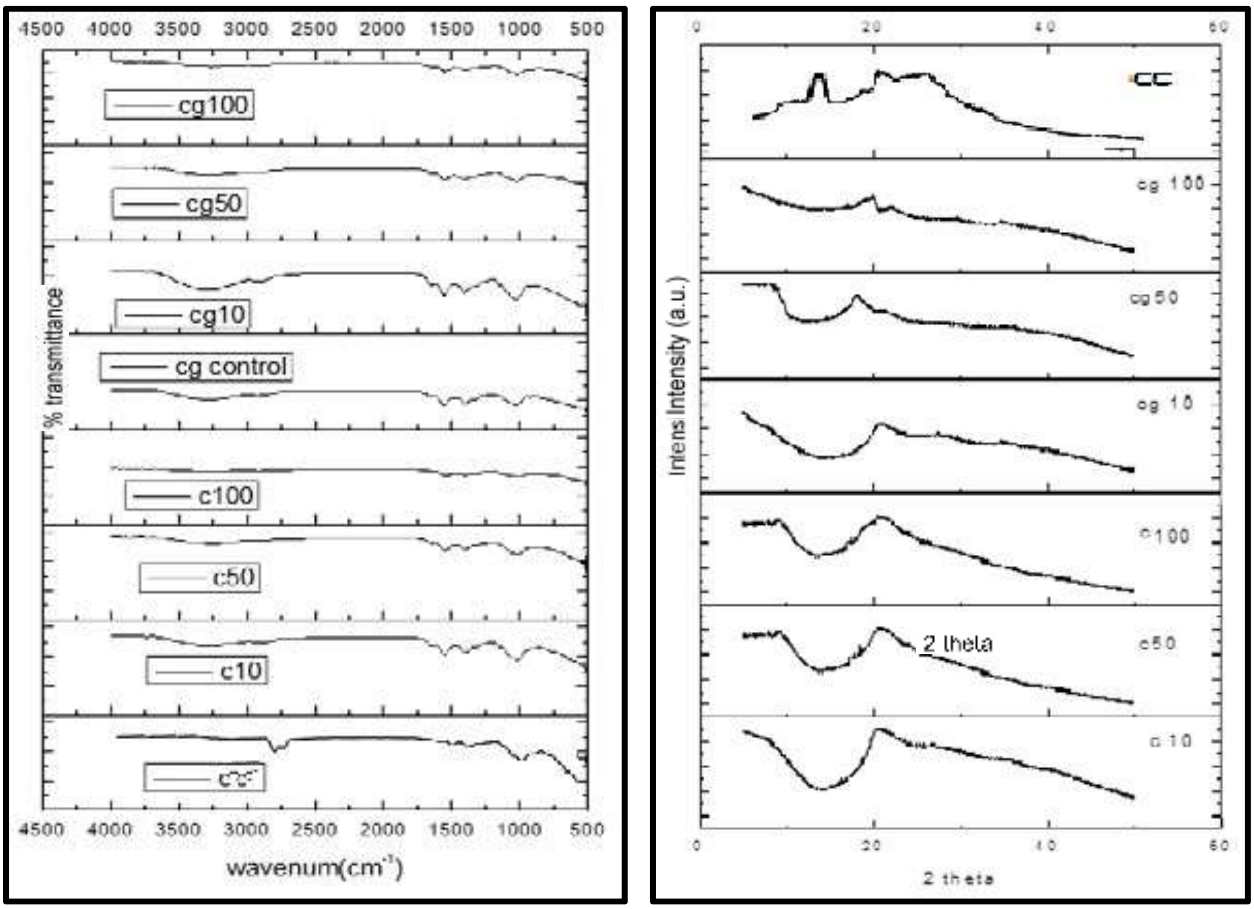

Figure 4.7 – *FTIR and XRD Spectrographs of chitosan-curcumin, chitosan-curcumin-glycerol films*

4.1.2.3 DRUG RELEASE KINETICS OF CURUMIN LOADED CHITOSAN COMPOSITE FILMS:

The drug release of the curcumin loaded chitosan films were carried out as seen in figure-4.8, there is steady release of curcumin from the chitosan films. The glycerol-cucumin chitosan films showed increase drug release this may be because the glycerol decreased the plasticity of the

formed films and the curcumin leached out from the matrix much faster than the chitosan-curcumin films. Overall there was noticed a steady increase in the release of curcumin.

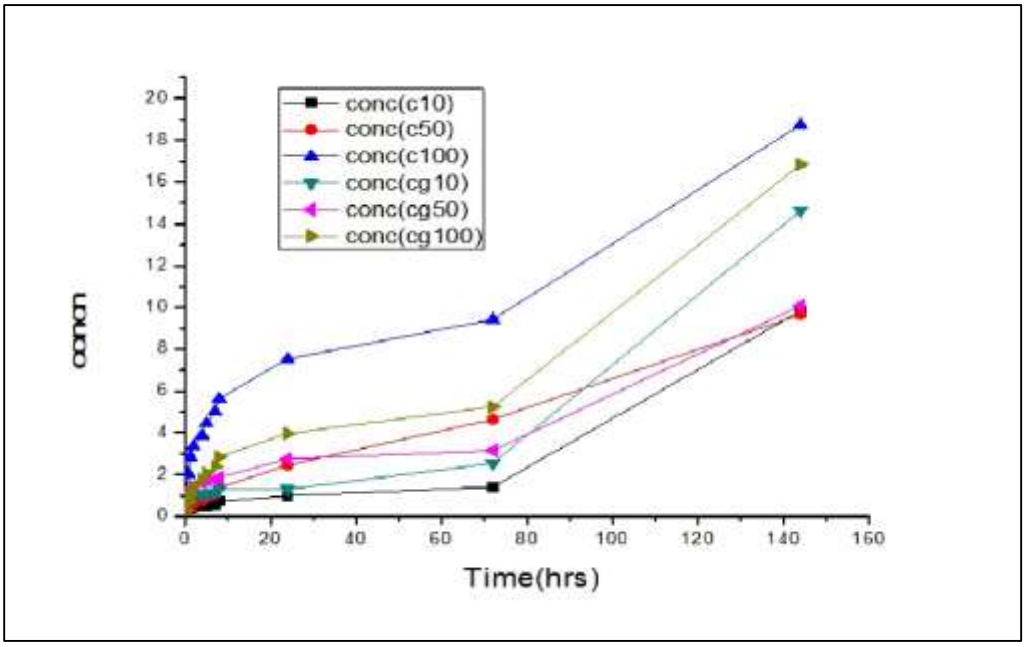

Figure 4.8 – *Drug release kinetics of the curcumin-chitosan and curcumin-chitosan-glycerol films*

4.1.2.4 HEMO-COMPATABILITY OF CURCUMIN COMPOSITE CHITOSAN FILMS:

The hemo-compatability of the curcumin-chitosan composite films were done using the goat blood and it was found that all the composite films were found to possess a percent hemolysis (%Z) which was less than 2. Thus all the films are hemo-compatible and can be successfully implied for wound healing applications as wound dressing materials. The Table-4.5 shows the hemo-compatibility results

Table 4.5 – *In vitro-hemo-compatibility test on curcumin-composite films*

Sample	OD Readings			Mean of OD(D_t)	Z%=(D_t-D_{nc})/ (D_{pc}-D_{nc})*100
	R1	R2	R3		
C control	0.225	0.225	0.225	0.225	1.611479
C 10	0.069	0.070	0.07	0.07	0
C 50	0.076	0.076	0.076	0.076	0
C 100	0.161	0.161	0.161	0.161	0.01
Cg	0.099	0.1	0.1	0.1	0
Cg10	0.066	0.066	0.066	0.066	0
Cg50	0.062	0.062	0.063	0.062	0
Cg100	0.049	0.049	0.049	0.049	0

4.1.2.5 *IN VITRO* CYTOTOXICITY TEST:

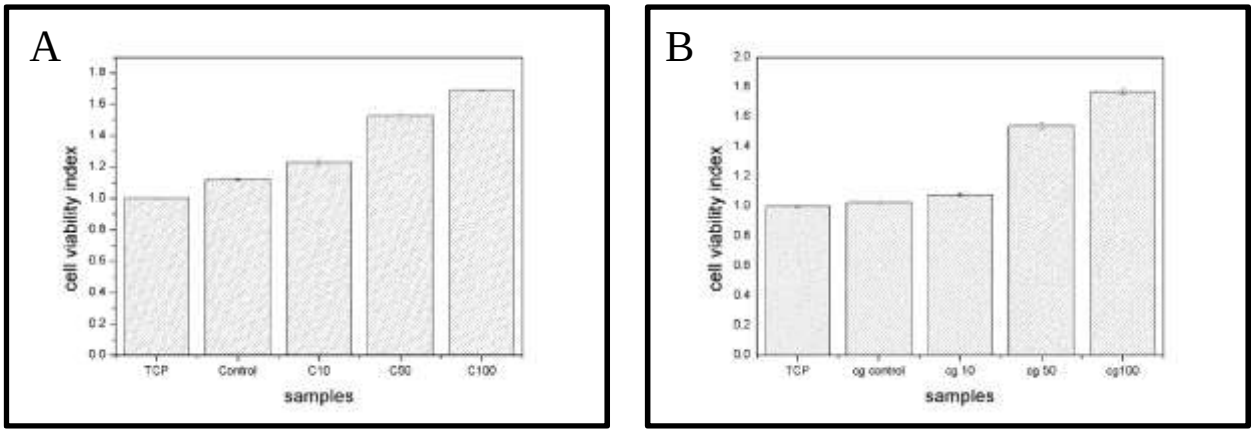

Figure 4.9 - *In vitro cyto-compatibility test using MTT for curcumin-chitosan and curcumin-chitosan-glycerol composite films*

It is seen that the curcumin-chitosan films enhanced the cellular metabolic activity of hADSCs and all the films were found to be cyto-compatible. With increase in concentration of curcumin concentration the cell viability also increased which proves the usefulness of the fabricated composite films can be successfully used as wound dressing material.

4.1.3 CHARACTERIZATION ALGINATE-CHITOSAN-ECM COMPOSITE FILMS:

4.1.3.1 MECHANICAL ANALYSIS OF THE ALGINATE-ECM-CHITOSAN FILMS:

Table 4.6 – *Mechanical Analysis of Chitosan Alginate ECM composite Films*

Specimen label	Specimen 1 chitosan	Specimen 2 alginate	Specimen 3 Chitosan alginate	Specimen 4 Chitosan alginate ECM
Maximum Load (N)	26.92	19.54	23.99	36.24
Tensile Strength (MPa)	53.84	65.13	59.96	60.41
Load at break (N)	20	17.39	22.63	29.15
Young`s Modulus (MPa)	2954.335	4270.911	2661.879	3554.288
Energy at Break (Standard) (J)	0.02516	0.00543	0.00855	0.01356
Extension at break	1.71296	0.53993	0.68450	0.58348
True Stress at break (standard)	43866994.659	59536199.738	58513683.033	49996013.272
True Strain at break (standard)	0.08218	0.02664	0.03365	0.02876

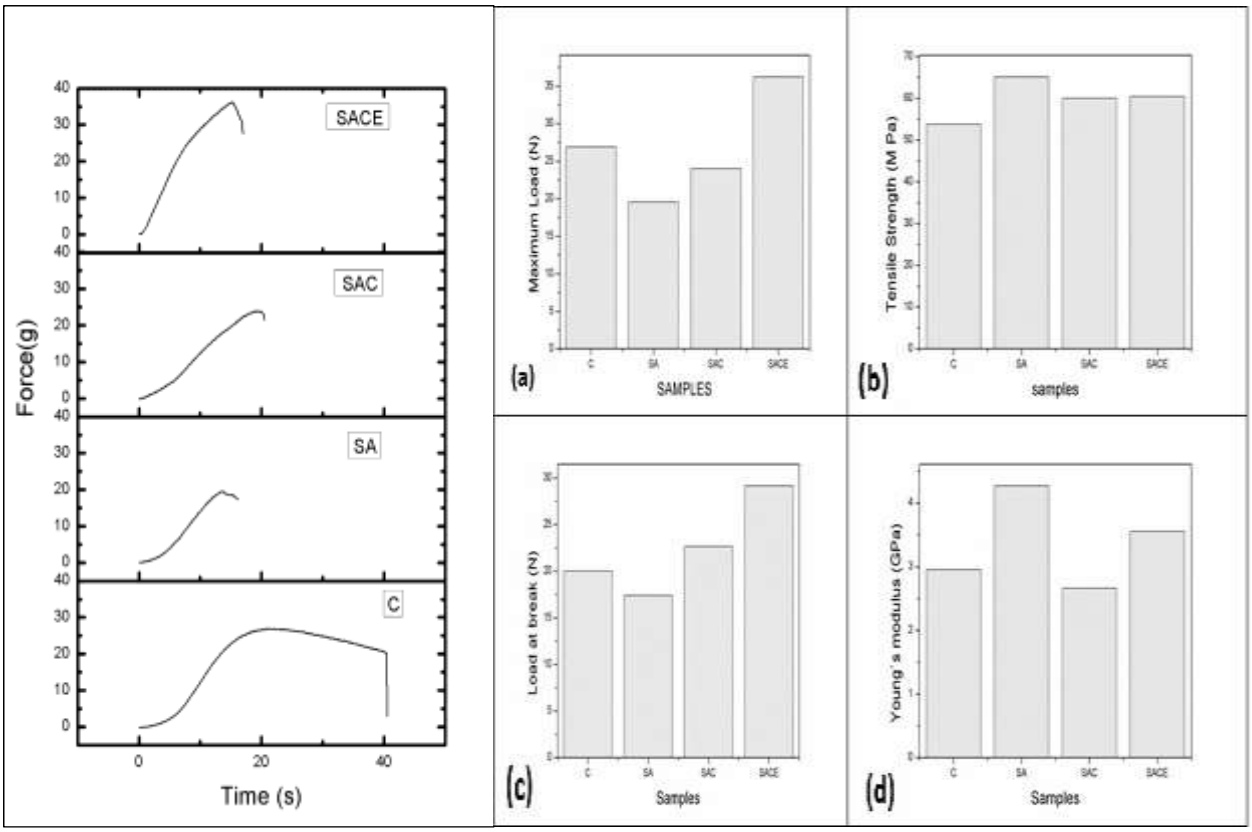

Figure 4.10 - *Mechanical analysis of alginate-chitosan-ECM composite films*

From Table-4.6 it is observed that with incorporation of ECM in the sodium-alginate films the ultimate tensile strength and the Young's modulus of the composite films increased when compared to the individual films of chitosan an alginate respectively. The ultimate tensile strength was found to be 60.41 MPa and its Young's modulus is found to be 3554 MPa.

4.1.3.2 WATER VAPOR TRANSMISSION TEST:

Water vapor transmission rate (WVTR) is regarded as the transmission of the water vapor per unit time through a unit area of the materials under test. The water vapor transmission rate (Table 4.7) was determined. The differences observed amongst the different groups were statistically significant. With incorporation of ECM concentration resulted in the decrease in the WVTR. The addition of ECM may result in increase of hydrophobicity and hence resulted in the decrease in the permeability of the water vapor from the films.

Table 4.7 – *Water vapor transmission rate*

SAMPLES	WATER VAPOUR TRANSMISSION RATE (g/day m^2)
Chitosan control (c)	3.341±1.12
Sodium Alginate(SA)	4.065±0.45
SA Chitosan(SAC)	3.358±0.61
SAC ECM(SACE)	2.686±0.82

4.1.3.3 XRD AND FTIR ANALYSIS:

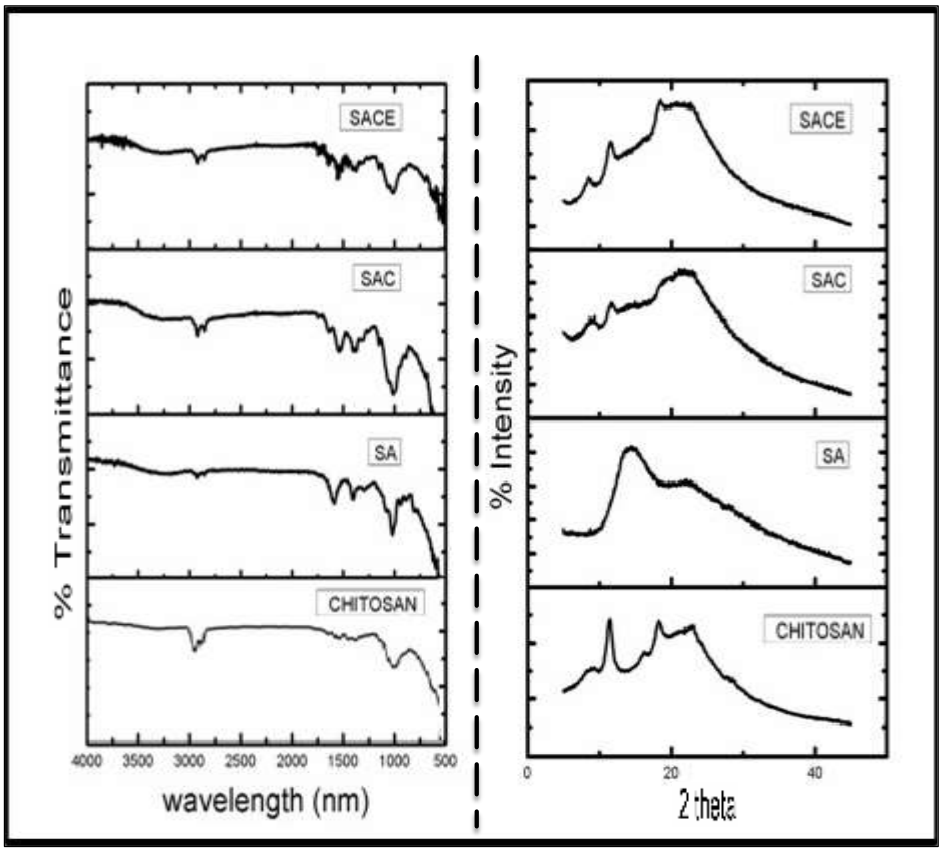

Figure 4.11 – *FTIR and XRD of chitosan-alginate ECM composite films*

From the FTIR spectrogram, it is observed that the peaks N-H & O-H stretching correspond to 3435 cm $^{-1}$, while CH_3 symmetric stretch occurs at 2956 cm^{-1}, the C=O stretching vibration is noticed at 1653 cm^{-1}, the C-O-C bending vibration occurs at 1126 cm^{-1}, the Amide I region is noticed at 1636-1660 cm^{-1} and Amide II bands at 1292 cm^{-1} for proteins. The incorporation of ECM in the sodium-alginate films was confirmed with the overlap of amide-I and II spectrsa in the composite films. From Figure-4.11, the XRD revealed a broad diffraction pattern at 10° 2θ and a characteristic peak at 23° 2θ for chitosan and typical peaks of chitosan in chitosan alginate – ECM found at 11.7° and 26.8° 2θ and similarly alginate exhibited a very small crystallinity at 12°, 23.1°, 31.3°,43.8°. The Crystallinity index for the films was calculated and it is as follows:

Table 4.8: *Crystallinity index of the films*

Samples	Crystallinity index
C	0.285
SA	0.2343
SAC	0.1382
SACE	0.2975

It is noticed that with incorporation of ECM the Crystallinity of the films increased and it is also seen from the XRD diffractogram.

4.1.3.4 *IN VITRO* CYTOTOXICITY TEST:

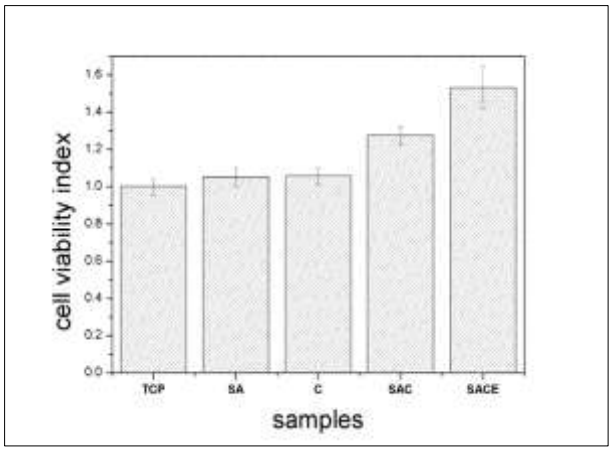

Figure 4.12 - *MTT for chitosan-alginate-ECM composite films*

All the films were found to be cytocompatible. The presence of ECM showed statistically significant increase in cellular proliferation than TCP (Tissue Culture Plate Control). The presence of protein 4.1 superfamily in extracellular matrix is known to increase the spreadability of the cells through integrin family receptor binding and β-integrin mediated cell spreading [30]. The results indicated that the developed composite films were well suited for wound healing applications.

4.2 PREPARATION AND CHARACTERIZATION OF POROUS SCAFFOLD:

4.2.1 XRD AND FTIR ANALYSIS:

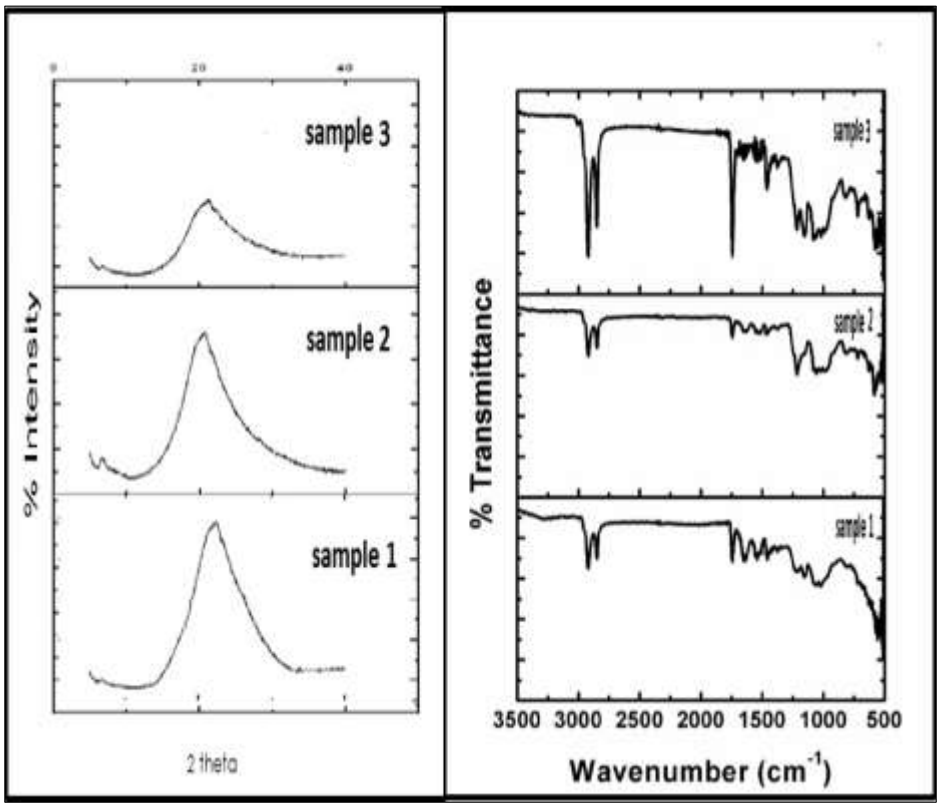

Figure 4.13 – *XRD and FTIR analysis of porous scaffolds; sample-1 is ECM, sample-2 is 0.1% Chitosan with ECM and sample-3 is 1% chitosan with ECM*

From the FTIR analysis the characteristic peaks of protein and chitosan were found as for Amide I region as seen in 1623-1643 cm^{-1} and Amide-II region between 1553-1578 cm^{-1} were noticed. For chitosan the CH_3 symmetric stretching was noticed at 2948 cm^{-1} whereas the CH_3 asymmetric bend at 1383 cm^{-1}, C-O-C bending at 1132 cm^{-1}, the CH stretching vibration at 1328

cm^{-1}, and the C-OH vibration at 1083 cm^{-1} were noticed. The successful incorporation of ECM was confirmed by the presence of Amide-I and Amide-II band at the composite films. The XRD results showed that the Crystallinity of the films decreased with increase in chitosan. The Crystallinity index of ECM sample, 0.1% chitosan-ECM and 1% chitosan ECM was found to be 0.745, 0.709 and 0.683 respectively.

4.2.2 SCANNING ELECTRON MICROSCOPY:

From Figure-4.14-B the presence of fat was noticed. If the porous ECM scaffold were washed with 0.5% SDS to remove fat, a better morphology of the scaffold can be obtained.

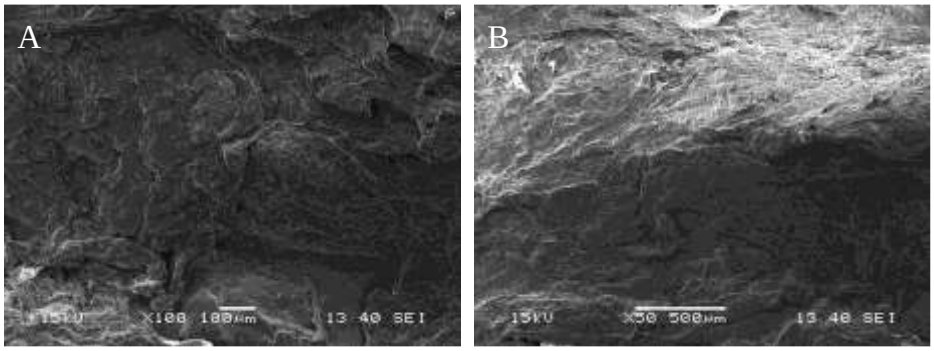

Figure 4.14 – *SEM Micrographs representing presence of fat in porous ECM scaffold*

From figure-4.15, it is observed that with increase in the chitosan concentration in the ECM-Chitosan composite scaffolds, the pore size gradually decreased. This is evident from the SEM micrographs and obviously chitosan plays a crucial role in controlling the porosity and the pore size of the freeze dried scaffold.

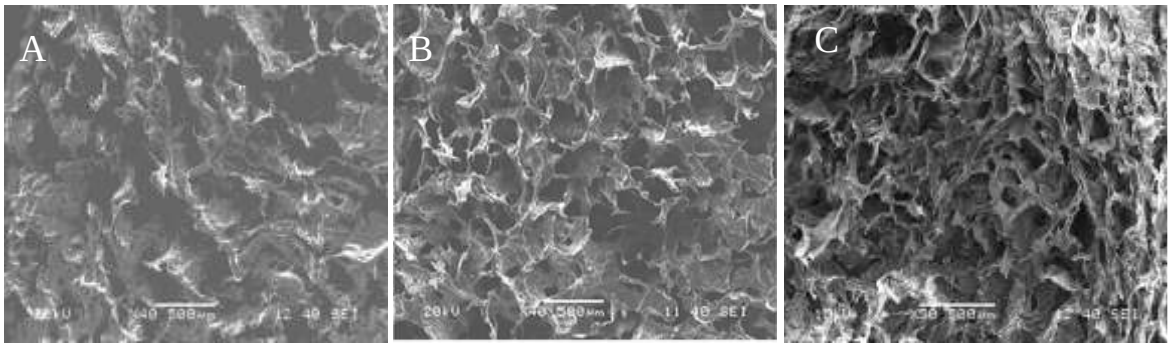

Figure 4.15 – *SEM micrographs of composite porous scaffolds; sample-1 is ECM, sample-2 is 0.1% Chitosan with ECM and sample-3 is 1% chitosan with ECM*

4.2.3 *IN VITRO* CYTOTOXICITY TEST:

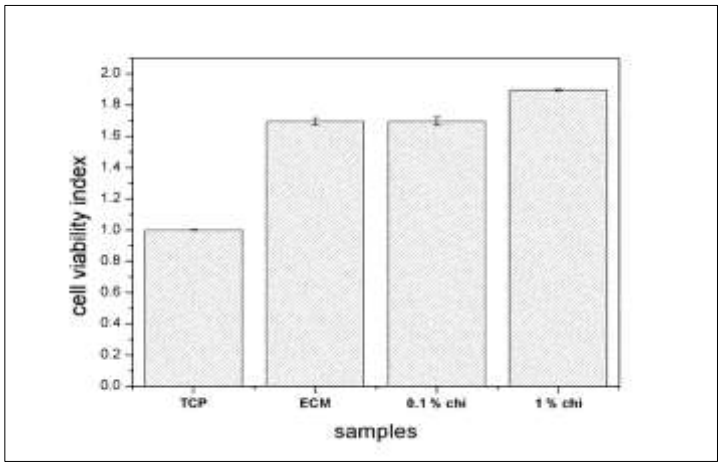

Figure 4.16 – *MTT assay for ECM, 0.1% Chitosan with ECM and 1% chitosan with ECM porous scaffolds*

All the samples were found to be cytocompatible. For all samples statistically significant increase in cellular proliferation ($p < 0.01$) when compared to the TCP (Tissue culture plate control) was noticed. No statistical significant difference($p<0.01$) in cellular proliferation between ECM and ECM+0.1% chitosan was observed. There was however statistical significant increase ($p<0.01$) in cellular proliferation in ECM+1% Chitosan when compared with ECM+0.1%Chitosan porous scaffold.

4.3 OPTIMIZATION OF PARAMETERS AND CHARACTERIZATION OF ALGINATE-ECM MICROBEADS:

4.3.1 OPTIMIZATION OF PARAMETERS:

Optimized parameters by taking the consideration of needle length between tip of the needle to the calcium chloride solution and at 3 % concentration of alginate, at different rpm. Finally, the optimized parameters at 1000 rpm in 15 ml falcon tube by taking 100 µm of calcium chloride with 0.1 % tween 80 at 3 % concentraion of alginate.

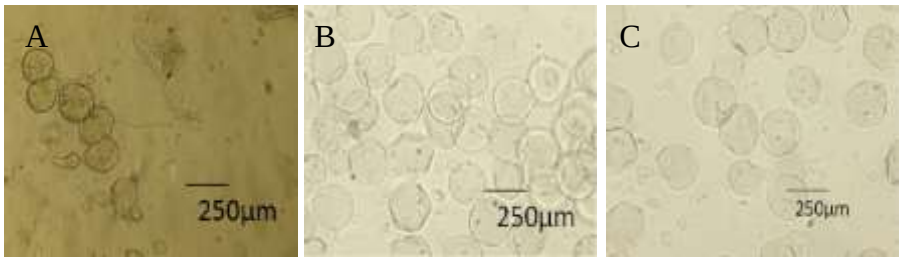

Figure 4.17 – *Optimized parameters and observed through optical microscopy*

A– with needle length, B-with 3000 rpm, C- with 2000 rpm

All these morphology through optical microscopy, the microbeads are not forming with the taylor cones and overlapping with each other.

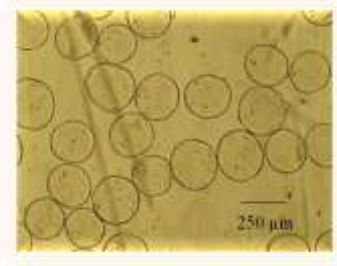

Figure 4.18 – *Optical microscope Image of sodium alginate ECM beads at 1000 rpm*

4.3.2 CONFOCAL MICROSCOPY :

The ECM can be detected by ANS (8-Annilino-napthalene sulfate) and observed that ECM can be incorporated into the micro beads and it is spherical.

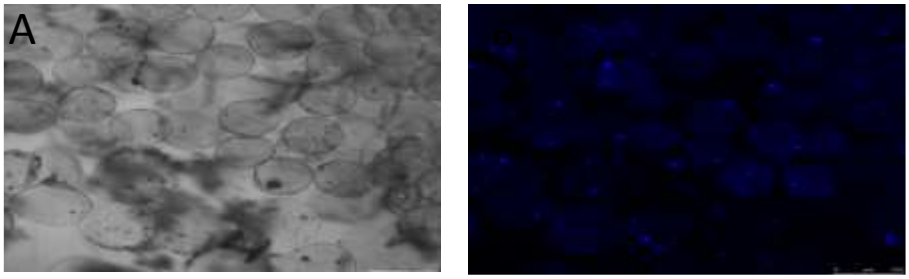

Figure 4.19 –*Confocal Microscopy Images of Sodium alginate ECM composite beads*

4.3.3 SCANNING ELECTRON MICROSCOPY:

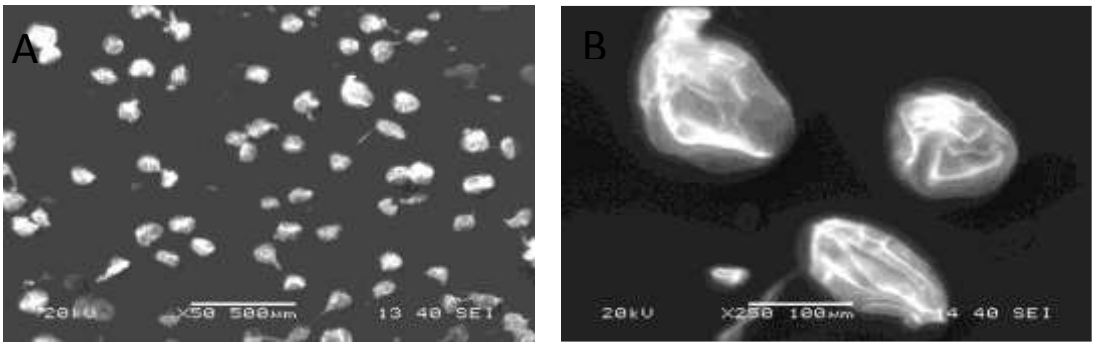

Figure 4.20 *SEM Images of dried sodium alginate ECM composite beads.*

The SEM results proved that ECM content can be within the beads even after drying of beads. In SEM analysis, observed that micro ridges and valleys which enhances the surface area.

4.3.4 X- RAY DIFFRACTION:

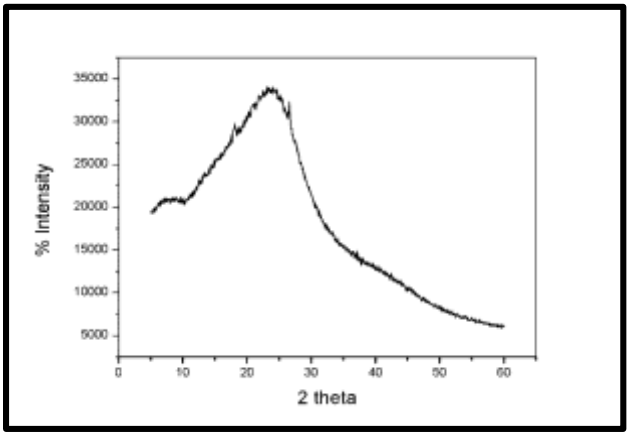

Figure 4.21 : *Analysis of XRD pattern of sodium alginate ECM composite microbeads*

The XRD analysis of sodium alginate ECM composite microbeads showed that the crystallinity index is 0.37813. According to literature review, found that the pure collagen and alginate execute broad peaks at 10°, 23° 2θ and the strong peak formation broaden due to introduction of ECM to alginate beads. It indicates increase in amorphous nature and decrease in crystallinity.

4.3.5 *IN VITRO* CYTOTOXICITY TEST:

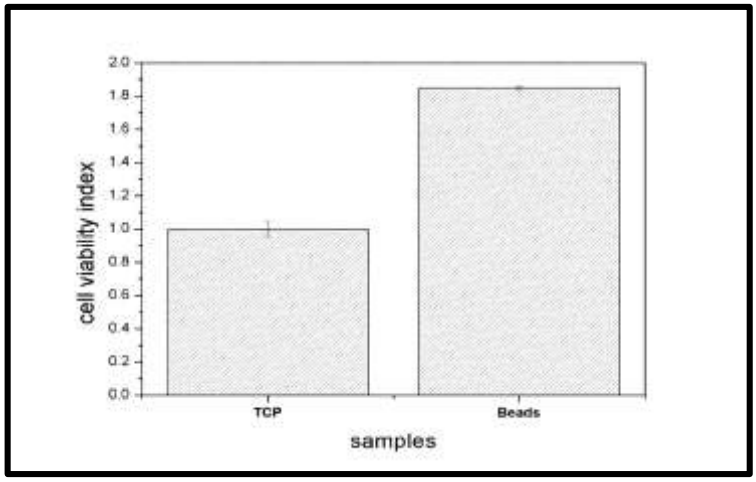

Figure 4.22 : *MTT assay of Sodium alginate ECM composite beads.*

The beads were found to be cytocompatible. There is statistically significant increase in cellular proliferation when compared to the TCP (Tissue culture plate control) was noticed.

4.4 OPTIMIZATION OF ECM COMPOSITE NANOFIBERS:

4.4.1 ECM – PVA ELECTROSPINNING OPTIMIZATION :

Electrospinning carried out in roller electrode electrospinning with the rpm range between 1-16 by varying the concentration of ECM in different solvents like distilled water, acetic acid (varying concentration) and NAOH (varying concentration) found that it is not electrospinnable. Later, tried with varying concentrations of both ECM and PVA (Poly Vinyl Alcohol) and by taking 10 % of PVA with varying concentration of SDS (Sodium Dodecyl Sulfate).

It was found that the solution is electrospinnable at 100 mg/ml with 10 % PVA and SDS at the concentration of 0.02 %.

Table 4.9 : *Optimizing the ECM PVA to generate fibers*

Sl No.	Solute	Solvent	Outcome
1	ECM(Varying conc.)	DW	Not electrospinnable
2	ECM(Varying conc.)	Acetic acid(varying conc.)	Not electrospinnable
3	ECM(Varying conc.)	NaOH(varying conc.)	Not electrospinnable
4	ECM(Varying conc.) + PVA(Varying conc.)	DW	Not electrospinnable
5	ECM(100 mg/ml) + PVA(10%) + less than 0.02% SDS	DW	Not electrospinnable
6	ECM(100 mg/ml) + PVA(10%) + 0.02% SDS or more	DW	Electrospinnable

Taking the optimized parameter in distilled water, tried with different distances between the sample and the collector at different voltage, at rpm 12 and measured the thickness.

Table 4.10 : *Electrospinning with ECM-PVA in optimized parameter.*

Sl No.	Distance (cm)	Voltage(kV)	Outcome	Thickness(nm)
1	11	< 45	Not Electrospinnable	-
2	11	≥45	Electrospinnable	375 ±56
3	12	≥45	Electrospinnable	225 ±25
4	13	<50	Not Electrospinnable	-
5	13	≥50	Electrospinnable	260±47
6	14	≥50	Electrospinnable	235±39
7	15	≥50	Electrospinnable	243±43
8	16	<55	Not Electrospinnable	-
9	16	≥55	Electrospinnable	198±28
10	17	≥55	Electrospinnable	213±56
11	18	≥55	Electrospinnable	235±65
12	19	≥55	Electrospinnable	527±84

Finally, optimized with the less thickness of fibers at 16 cm of distance at greater than or equal to 55 kV which is electrospinnable.

4.4.2 CHITOSAN ECM PVA ELECTROSPINNING OPTIMIZATION:

To exclude the SDS, tried with the chitosan – ECM – PVA composites electrospinning in the solvent of 0.5 M acetic acid.

Table 4.11 *: Optimizing with ECM Chitosan PVA in acetic acid solvent.*

Sl No.	Solute	Solvent	Outcome
1.	ECM(100 mg/ml)+PVA(10%)	0.5M acetic acid	Not Electrospinnable
2	{ECM(100 mg/ml)+PVA(10%) } : Chitosan (1%)=In varying ratio	0.5M acetic acid	Not Electrospinnable
3	{ECM(100 mg/ml)+PVA(10%) } : Chitosan (2%) = ≤ (40:60)	0.5M acetic acid	Not Electrospinnable
4	{ECM(100 mg/ml)+PVA(10%) } : Chitosan (2%) = 30:70	0.5M acetic acid	Electrospinnable
5	{ECM(100 mg/ml)+PVA(10%) } : Chitosan (2%) = ≥ (20:80)	0.5M acetic acid	Not Electrospinnable

Finally, the composite with chitosan at the concentration of 100 mg/ml of ECM, 10 % of PVA and at concentration of 2 % chitosan in 30 : 80 ratio nanofibers were obtained.

By taking the above optimized parameter, tried at different distances and voltages to obtain less thickness of fibers.

Table 4.12: *Optimizing working distance for nanofiber generation*

Distance (cm)	Voltage(kV)	Outcome	Thickness (nm)
11	<55	Not Electrospinnable	-
11	≥55	Electrospinnable	544±57
13	<55	Not Electrospinnable	-
13	≥55	Electrospinnable	356±65
15	<55	Not Electrospinnable	-
15	≥55	Electrospinnable	410±48
17	<60	Not Electrospinnable	-
17	≥60	Electrospinnable	586±76

At the working distance of 13 cm and the working voltage at greater than or equal to 55 obtained less thickness of nano fibers.

4.4.3 SCANNING ELECTRON MICROSCOPY:

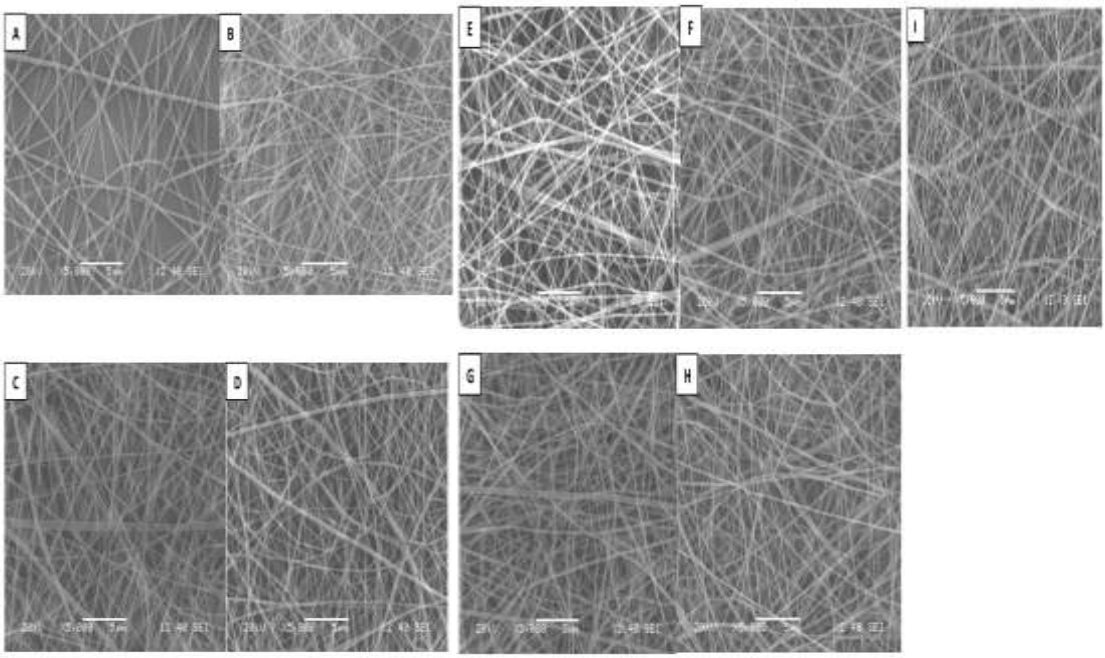

Figure 4.23 : *SEM Micrographs of nano fibers with ECM PVA composite.*

A: PVA-SDS-ECM:11 cm

B: PVA-SDS-ECM:12 cm

C: PVA-SDS-ECM:13 cm

D: PVA-SDS-ECM:14 cm

E: PVA-SDS-ECM:15 cm

F: PVA-SDS-ECM:16 cm

G: PVA-SDS-ECM:17 cm

H: PVA-SDS-ECM:18 cm

I : PVA-SDS-ECM:19 cm

The Electrospinning with PVA-SDS-ECM nanofibers obtained with less thickness at 16 cm of working distance.

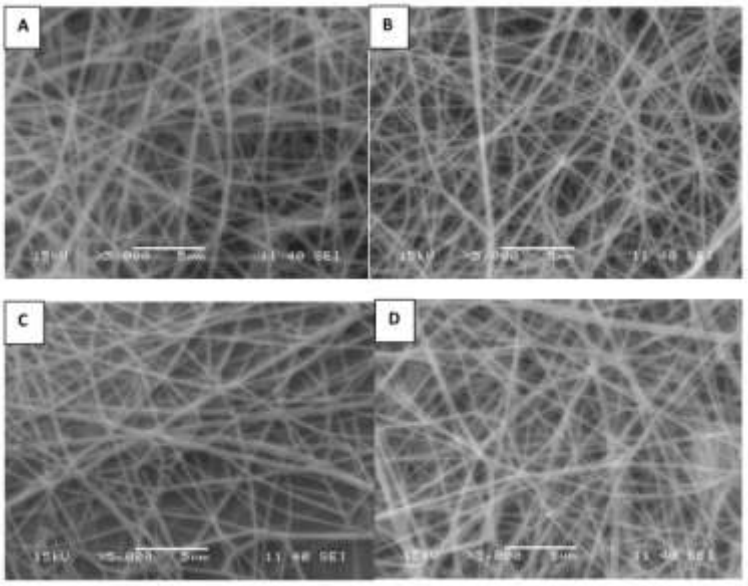

Figure 4.24 : *SEM micrographs of nanofibers with chitosan – ECM – PVA composite.*

A : Chitosan-PVA-ECM (11 cm- 55kV)

B : Chitosan-PVA-ECM (13 cm- 55kV)

C : Chitosan-PVA-ECM (15 cm -55 kV)

D : Chitosan-PVA-ECM (17 cm - 60kV)

The electrospinning of ECM-PVA- chitosan nanofibers obtained with less thickness at working distance of 13 cm.

CHAPTER-5

CONCLUSION

The present study reports the preparation and characterization of the human derived ECM and chitosan composite films, chitosan ECM porous scaffolds, ECM PVA chitosan nanofibers and sodium alginate chitosan ECM beads. An increase in the chitosan content resulted in decrease in pore size and crystallinity of porous scaffolds. Alginate beads with ECM can be prepared for soft tissue engineering within 250 µm, at 1000 rpm. Nanofibers can be formed with less thickness by optimizing the parameters of chitosan ECM PVA in acetic acid. An increase in the ECM content resulted in the increase in the hydrophilicity of the films. This, in turn, was found to improve the moisture retention capacity and prevent the evaporation of water. This is important in wound healing. Excessive evaporation of water results in the drying of the wound surface, which subsequently results in the decrease in the biosynthetic reactions occurring at the wound surface. This consequently results in the decrease in the wound healing rate. The mechanical studies suggested that the films with higher proportions of ECM (within the experimental compositions) may be more efficient as wound dressing materials. The presence of ECM did not alter the hemolysis significantly. Though metabolic assay results indicate decrease in cell proliferation in presence of ECM, the metabolic assay indices are still quite higher than the petri dishes (control). The preliminary study suggested a positive sign that the ECM based composites along with chitosan may be tried as wound dressing materials. In future, the efficacy of the human ECM and the composite films will be evaluated in chronic wounds *in vivo*.

REFERENCES

[31]

1. Diegelmann, R.F. and M.C. Evans, *Wound healing: an overview of acute, fibrotic and delayed healing.* Front Biosci, 2004. **9**(1): p. 283-289.
2. Huss, R., et al., *PLURIPOTENCY OF ADULT STEM CELLS.*
3. Kishida, A. and Y. Ikada, *Hydrogels for biomedical and pharmaceutical applications.* Polymeric biomaterials, 2001: p. 133Ğ145.
4. Brett, D., *A review of collagen and collagen-based wound dressings.* Wounds-A compendium of clinical research and practice, 2008. **20**(12): p. 347-356.
5. Sorokin, L., *The impact of the extracellular matrix on inflammation.* Nature Reviews Immunology, 2010. **10**(10): p. 712-723.
6. Cartier, R., et al., *Angiogenic factor: a possible mechanism for neovascularization produced by omental pedicles.* The Journal of thoracic and cardiovascular surgery, 1990. **99**(2): p. 264-268.
7. Saltz, R., et al., *Laparoscopically harvested omental free flap to cover a large soft tissue defect.* Annals of surgery, 1993. **217**(5): p. 542.
8. Azad, A.K., et al., *Chitosan membrane as a wound-healing dressing: Characterization and clinical application.* Journal of Biomedical Materials Research Part B: Applied Biomaterials, 2004. **69**(2): p. 216-222.
9. Archana, D., et al., *Chitosan-PVP-nano silver oxide wound dressing: In vitro and in vivo evaluation.* International Journal of Biological Macromolecules, 2015. **73**(0): p. 49-57.
10. Zhu, Y., et al., *Collagen–chitosan polymer as a scaffold for the proliferation of human adipose tissue-derived stem cells.* Journal of Materials Science: Materials in Medicine, 2009. **20**(3): p. 799-808.
11. Xu, H., et al., *Chitosan–hyaluronic acid hybrid film as a novel wound dressing: in vitro and in vivo studies.* Polymers for Advanced Technologies, 2007. **18**(11): p. 869-875.
12. Gu, Z., et al., *Preparation of chitosan/silk fibroin blending membrane fixed with alginate dialdehyde for wound dressing.* International journal of biological macromolecules, 2013. **58**: p. 121-126.
13. Nguyen, V.C., V.B. Nguyen, and M.-F. Hsieh, *Curcumin-loaded chitosan/gelatin composite sponge for wound healing application.* International Journal of Polymer Science, 2013. **2013**.
14. Nazarov, R., H.-J. Jin, and D.L. Kaplan, *Porous 3-D scaffolds from regenerated silk fibroin.* Biomacromolecules, 2004. **5**(3): p. 718-726.
15. Mansur, H.S. and H.S. Costa, *Nanostructured poly (vinyl alcohol)/bioactive glass and poly (vinyl alcohol)/chitosan/bioactive glass hybrid scaffolds for biomedical applications.* Chemical Engineering Journal, 2008. **137**(1): p. 72-83.
16. Kumar, M.N.R., *A review of chitin and chitosan applications.* Reactive and functional polymers, 2000. **46**(1): p. 1-27.
17. Blair, H.S., et al., *Chitosan and modified chitosan membranes I. Preparation and characterisation.* Journal of Applied Polymer Science, 1987. **33**(2): p. 641-656.

18. Miller, J.S., et al., *Successful adoptive transfer and in vivo expansion of human haploidentical NK cells in patients with cancer.* Blood, 2005. **105**(8): p. 3051-3057.
19. Gelse, K., E. Pöschl, and T. Aigner, *Collagens—structure, function, and biosynthesis.* Advanced drug delivery reviews, 2003. **55**(12): p. 1531-1546.
20. Kouchak, M., et al., *Chitosan and polyvinyl alcohol composite films containing nitrofurazone: preparation and evaluation.* Iranian journal of basic medical sciences, 2014. **17**(1): p. 14.
21. Woessner, J., *The determination of hydroxyproline in tissue and protein samples containing small proportions of this imino acid.* Archives of biochemistry and biophysics, 1961. **93**(2): p. 440-447.
22. Li, X., et al., *In vivo evaluation of curcumin nanoformulation loaded methoxy poly (ethylene glycol)-graft-chitosan composite film for wound healing application.* Carbohydrate Polymers, 2012. **88**(1): p. 84-90.
23. Remunan-Lopez, C. and R. Bodmeier, *Mechanical, water uptake and permeability properties of crosslinked chitosan glutamate and alginate films.* Journal of controlled release, 1997. **44**(2): p. 215-225.
24. Häuselmann, H., et al., *Synthesis and turnover of proteoglycans by human and bovine adult articular chondrocytes cultured in alginate beads.* Matrix, 1992. **12**(2): p. 116-129.
25. Tao, J. and S. Shivkumar, *Molecular weight dependent structural regimes during the electrospinning of PVA.* Materials letters, 2007. **61**(11): p. 2325-2328.
26. Bellido, G. and D. Hatcher, *Asian noodles: Revisiting Peleg's analysis for presenting stress relaxation data in soft solid foods.* Journal of food engineering, 2009. **92**(1): p. 29-36.
27. AbdElhady, M., *Preparation and characterization of chitosan/zinc oxide nanoparticles for imparting antimicrobial and UV protection to cotton fabric.* International journal of carbohydrate chemistry, 2012. **2012**.
28. Sundarrajan, P., et al., *One pot synthesis and characterization of alginate stabilized semiconductor nanoparticles.* Bulletin of the Korean Chemical Society, 2012. **33**(10): p. 3218-3224.
29. Wu, Y.-B., et al., *Preparation and characterization on mechanical and antibacterial properties of chitsoan/cellulose blends.* Carbohydrate Polymers, 2004. **57**(4): p. 435-440.
30. Jung, Y. and J.H. McCarty, *Band 4.1 proteins regulate integrin-dependent cell spreading.* Biochemical and biophysical research communications, 2012. **426**(4): p. 578-584.
31. Archana, D., et al., *Chitosan-PVP-nano silver oxide wound dressing: In vitro and in vivo evaluation.* International journal of biological macromolecules, 2015. **73**: p. 49-57.